Neutrinoless double beta decay in a left-right symmetric model with a double seesaw mechanism

Sudhanwa Patra,[1,*] S. T. Petcov,[2,3,†] Prativa Pritimita,[4,‡] and Purushottam Sahu[1,2,5,§]

[1]*Department of Physics, Indian Institute of Technology Bhilai, Raipur 492015, India*
[2]*SISSA/INFN, Via Bonomea 265, 34136 Trieste, Italy*
[3]*Kavli IPMU (WPI), UTIAS, The University of Tokyo, Kashiwa, Chiba 277-8583, Japan*
[4]*Department of Physics, Indian Institute of Technology Bombay, Powai, Mumbai 400076, India*
[5]*International Centre for Theoretical Physics (ICTP), Strada Costiera 11, Trieste 34151, Italy*

(Received 6 March 2023; accepted 5 April 2023; published 26 April 2023)

We discuss a left-right (L-R) symmetric model with the double seesaw mechanism at the TeV scale generating Majorana masses for the active left-handed (LH) flavor neutrinos $\nu_{\alpha L}$ and the heavy right-handed (RH) neutrinos $N_{\beta R}, \alpha, \beta = e, \mu, \tau$, which in turn mediate lepton number violating processes, including neutrinoless double beta decay. The Higgs sector is composed of two Higgs doublets H_L, H_R, and a bidoublet Φ. The fermion sector has the usual for the L-R symmetric models quarks and leptons, along with three $SU(2)$ singlet fermion $S_{\gamma L}$. The choice of bare Majorana mass term for these sterile fermions induces large Majorana masses for the heavy RH neutrinos leading to two sets of heavy Majorana particles N_j and $S_k, j, k = 1, 2, 3$, with masses $m_{N_j} \ll m_{S_k}$. Working with a specific version of the model in which the $\nu_{\alpha L} - N_{\beta R}$ and the $N_{\beta R} - S_{\gamma L}$ Dirac mass terms are diagonal, and assuming that $m_{N_j} \sim$ (1–1000) GeV and $\max(m_{S_k}) \sim$ (1–10) TeV, $m_{N_j} \ll m_{S_k}$, we study in detail the new "nonstandard" contributions to the $0\nu\beta\beta$ decay amplitude and half-life arising due to the exchange of virtual N_j and S_k. We find that in both cases of NO and IO light neutrino mass spectra, these contributions are strongly enhanced and are dominant at relatively small values of the lightest neutrino mass $m_{1(3)} \sim (10^{-4}$–$10^{-2})$ eV over the light Majorana neutrino exchange contribution. In large part of the parameter space, the predictions of the model for the $0\nu\beta\beta$ decay generalized effective Majorana mass and half-life are within the sensitivity range of the planned next generation of neutrinoless double beta decay experiments LEGEND-200 (LEGEND-1000), nEXO, KamlAND-Zen-II, CUPID, and NEXT-HD.

DOI: 10.1103/PhysRevD.107.075037

I. INTRODUCTION

Neutrino mass and mixing, which was confirmed by oscillation experiments [1–5] cannot be understood within the Standard Model (SM) of particle physics since it predicts massless neutrinos. So, there has to be a mechanism beyond the SM which generates nonzero mass for these tiny particles. The seesaw mechanism has become quite famous for explaining the same by extending the SM in the minimal possible way. Some of the variants of this mechanism are type-I [6–9], type-II [10–14], and type-III [15,16] seesaw which can be achieved by adding a right-handed (RH) neutrino, a scalar triplet, and a fermion triplet to the SM respectively. However, a heavy right-handed scale associated with these seesaw mechanisms renders them unverifiable at the collider experiments. Thus, the necessity arises to bring down the seesaw scale to a verifiable TeV range. The seesaw mechanisms assume neutrinos are Majorana particles, which can be probed via the lepton number violating (LNV) process of neutrinoless double beta decay [17]. Such a rare transition occurs when two neutrons simultaneously decay into two protons and two electrons without any neutrinos. It can be induced either by light left-handed neutrinos, called the standard mechanism or by exotic particles like heavy right-handed neutrinos or sterile neutrinos, called new physics contribution. In the standard mechanism case, the experimental limits on the half-life of the decay can only be saturated by quasidegenerate [18] light neutrinos, which are disfavored by cosmological data sets [19–22]. On the other

*sudhanwa@iitbhilai.ac.in
†Also at Institute of Nuclear Research and Nuclear Energy, Bulgarian Academy of Science, 1784 Sofia, Bulgaria.
‡prativa@iitb.ac.in
§psahu@ictp.it

hand, identifying the correct neutrino mass hierarchy, considering the sum of light neutrino masses, would require a multiton scale detector that is beyond feasible in the near future. Any comparative future experimental observation of $0\nu\beta\beta$ decay would only be attributed to new physics contribution. The current lower limit on the decay half-life of Ge^{76} is $T^{0\nu}_{1/2} > 1.8 \times 10^{26}$ yrs at 90% C.L. from GERDA [23]. Experiments using the isotope Xe^{136} like EXO-200 [24] and KamLAND-Zen [25,26] have derived lower bounds on the half-life as $T^{0\nu}_{1/2} > 3.5 \times 10^{25}$ yrs and $T^{0\nu}_{1/2} > 1.07 \times 10^{26}$, yrs respectively. With this motivation, we consider a left-right symmetric model with a double seesaw mechanism [27,28] as new physics and study the new contributions to $0\nu\beta\beta$ decay process.

The left-right symmetric model (LRSM) [29–32] is a well-suited candidate for physics beyond SM for several reasons. To name a few, it can explain the theoretical origin of maximal parity violation in weak interaction, it can incorporate neutrino mass due to the presence of a right-handed neutrino state, it appears as a subgroup of SO(10) Grand Unified Theory, and it can be broken down to SM gauge symmetry at low energies. Moreover, it delivers rich phenomenology if the left-right symmetry breaking occurs at few TeV scale [33–63]. The spontaneous symmetry breaking of left-right symmetric model (LRSM) to SM plays a vital role in generating neutrino mass through the seesaw mechanism. The seesaw scheme varies with the choice of scalars considered in the left-right model and regulates the associated phenomenology. In general, symmetry breaking can be done with the help of Higgs doublets or Higgs triplets or with the combination of both doublets and triplets. In the case of Higgs doublets, neutrinos do not get Majorana mass, and thus the model forbids any signatures of lepton number violation or lepton flavor violation (LFV). In the case of Higgs triplets, neutrino mass is generated via the type-I plus type-II seesaw mechanism. Even though Majorana mass is generated for light and heavy neutrinos in this case, the seesaw cannot be probed by experiments considering the high scale associated with it.

The seesaw scale can be brought down to the TeV range in the case of a linear seesaw and inverse seesaw, some of which are discussed in Refs. [53,64–72]. However, in the case of a linear seesaw and inverse seesaw the light neutrinos are Majorana. In contrast, the heavy neutrinos are pseudo-Dirac, due to which the heavy neutrinos do not play a dominant role in lepton number violation. To study dominant new contributions to LNV and LFV decays, the Higgs and fermion sectors of LRSM have been extended in Refs. [73–77].

We explore here a double seesaw mechanism [27,28] within a left-right symmetric model without Higgs triplets allowing significant lepton number violation and new physics contribution to neutrinoless double beta decay. We keep the scalar sector of the model minimal while adding only one sterile neutrino per generation in the fermion sector. Even though the Higgs and fermion sectors are the same as in the case of a linear and inverse seesaw, the choice of bare Majorana masses for sterile neutrinos can induce large Majorana masses for heavy RH neutrino as well. The nonzero masses for RH neutrinos are generated through the double seesaw mechanism by implementing seesaw approximation twice. In the first step, the Majorana mass matrix and masses of the RH neutrinos are generated via the type-I seesaw mechanism. In this case, light neutrino mass becomes linearly dependent on a heavy sterile neutrino mass scale. This is how the double seesaw mainly differs from the canonical seesaw mechanism, where the light neutrino masses are inversely proportional to heavy RH neutrino masses. Another essential feature of our model is that we express mass relations between light and heavy Majorana neutrinos in terms of oscillation parameters and the lightest neutrino mass. Thus, it enables us to derive meaningful information about the absolute scale of the lightest neutrino mass and mass hierarchy from the new contributions to the neutrinoless double beta decay process by saturating the current experimental limits.

The plan of the paper can be summarized as follows. In Sec. II, we give a brief description of the left-right symmetric model with the double seesaw mechanism. In Sec. III we explain the implementation of the double seesaw mechanism and the origin of Majorana masses for light and heavy right-handed (RH) and sterile neutrinos. The generation of the masses of gauge bosons associated with the $SU(2)_R$ gauge group as well the constraints on their masses and on their mixing with the Standard Model gauge bosons are also considered in this section. The general expression for the neutrinoless double beta decay half-life, including the new physics (i.e., the "nonstandard") contributions is given in Sec. IV, in which we also, present and discuss briefly the nuclear matrix elements of the process and their current uncertainties. Detailed phenomenological analysis of the nonstandard contributions together with numerical estimates of their magnitude are presented in Sec. V. We also give predictions of the considered model for the neutrinoless double beta decay "generalized" effective Majorana mass and half-life accounting, in particular, for the uncertainties of the relevant nuclear matrix elements. Section VI contains brief comments on the potential lepton flavor violation and collider phenomenology of the considered model. Section VII contains a summary of the results obtained in the present study. In the Appendix, we give a detailed derivation of the masses and mixing of the light and heavy Majorana neutrinos in the considered left-right symmetric model with a double seesaw mechanism of neutrino mass generation.

II. LEFT-RIGHT SYMMETRIC MODEL WITH DOUBLE SEESAW

Left-Right symmetric models were proposed with the motivation of restoring parity (or left-right) symmetry at a high scale [29–32]. Therefore, in the model the left- and right-handed fermion fields are assigned to $SU(2)_L$ and $SU(2)_R$ doublets, respectively, which are related by a discrete symmetry. The complete gauge group, which is an extension of the SM gauge group can be written as

$$\mathcal{G}_{LR} \equiv SU(2)_L \times SU(2)_R \times U(1)_{B-L}, \tag{2.1}$$

where $SU(3)_C$ is omitted for simplicity. The electric charge for any particle in this model is defined as

$$Q = T_{3L} + T_{3R} + \frac{B-L}{2}, \tag{2.2}$$

where T_{3L} (T_{3R}) is the third component of the isospin associated with the $SU(2)_L$ ($SU(2)_R$) gauge group. The model's fermion sector comprises all the Standard Model fermions plus a right-handed neutrino N_R. The fermion fields with their respective quantum numbers can be written as follows:

$$q_L = \begin{pmatrix} u_L \\ d_L \end{pmatrix} \equiv [2,1,1/3], \qquad q_R = \begin{pmatrix} u_R \\ d_R \end{pmatrix} \equiv [1,2,1/3],$$
$$\ell_L = \begin{pmatrix} \nu_L \\ e_L \end{pmatrix} \equiv [2,1,-1], \qquad \ell_R = \begin{pmatrix} N_R \\ e_R \end{pmatrix} \equiv [1,2,-1].$$

The scalar sector is responsible for the spontaneous symmetry breaking of LRSM to SM and plays a crucial role in deciding the type of seesaw mechanism through which neutrino masses can be generated. The left-right symmetry breaking can be done either with the help of doublets H_L, H_R, or triplets Δ_L, Δ_R, or with the combination of both doublets and triplets. The next step of symmetry breaking, i.e., the breaking of SM symmetry to $U(1)_{em}$, is done with the help of the doublet ϕ contained in the bidoublet Φ. The doublets H_L, H_R, and the bidoublet Φ have the form,

$$H_L = \begin{pmatrix} h_L^+ \\ h_L^0 \end{pmatrix} \equiv [2,1,1],$$
$$H_R = \begin{pmatrix} h_R^+ \\ h_R^0 \end{pmatrix} \equiv [1,2,1],$$
$$\Phi = \begin{pmatrix} \phi_1^0 & \phi_2^+ \\ \phi_1^- & \phi_2^0 \end{pmatrix} \equiv [2,2,0], \tag{2.3}$$

The symmetry breaking steps can be sketched as follows:

Spontaneous symmetry breaking of LRSM:

$$\underbrace{\underset{\{T_L,T_{3L}\}}{SU(2)_L} \times \underset{\{T_R,T_{3R}\}}{SU(2)_R} \times \underset{B-L}{U(1)_{B-L}}}_{\substack{g_L \quad g_R \quad g_{BL} \\ \downarrow \langle H_R(1,2,1)\rangle}}$$
$$\underbrace{\underset{\{T_L,T_{3L}\}}{SU(2)_L} \times \underset{Y}{U(1)_Y}}_{\substack{g \equiv g_L \quad g' \\ \downarrow \langle \phi(1_L,1/2_Y)\rangle \subset \Phi(2_L,2_R,0_{B-L})}}$$
$$\underset{(Q,\,e)\quad Q=T_{3L}+Y}{U(1)_{em}}$$

The first step of symmetry breaking, i.e., $SU(2)_R \times U(1)_{B-L} \to U(1)_Y$ is achieved by assigning a nonzero vacuum expectation value (VEV) $\langle H_R^0 \rangle$ to the neutral component h_R^0 of H_R as v_R. The scale of this symmetry breaking determines the mass of the heavily charged and neutral gauge bosons associated with the $SU(2)_R$ symmetry, W_R and Z_R. The scalar doublet H_L doesn't play any role but is present because of the left-right invariance. The electroweak symmetry breaking i.e., $SU(2)_L \times U(1)_Y \to U(1)_{em}$, is done by assigning nonzero VEVs $\langle \phi_1^0 \rangle \equiv v_1$ and $\langle \phi_2^0 \rangle \equiv v_2$ to the neutral components of Φ, with $v_{\rm SM} = \sqrt{v_1^2 + v_2^2} \simeq 246$ GeV. The neutral components of the scalar bidoublet generate masses for the quarks and charged leptons via the following Yukawa Lagrangian,

$$-\mathcal{L}_{Yuk} \supset \overline{q_L}[Y_1\Phi + Y_2\tilde{\Phi}]q_R + \overline{\ell_L}[Y_3\Phi + Y_4\tilde{\Phi}]\ell_R + \text{H.c.}, \tag{2.4}$$

where $\tilde{\Phi} = \sigma_2 \Phi^* \sigma_2$ and σ_2 is the second Pauli matrix. When the scalar bidoublet Φ acquires nonzero VEVs,

$$\langle \Phi \rangle = \begin{pmatrix} v_1 & 0 \\ 0 & v_2 \end{pmatrix}, \tag{2.5}$$

it gives masses to quarks and charged leptons in the following manner:

$$M_u = Y_1 v_1 + Y_2 v_2,$$
$$M_d = Y_1 v_2 + Y_2 v_1,$$
$$M_e = Y_3 v_2 + Y_4 v_1. \tag{2.6}$$

Here M_u (M_d) and M_e are the up-type (down-type) quark and charged lepton-mass matrices. The Lagrangian in Eq. (2.4) also yields Dirac mass for the light neutrinos as

$$M_D^\nu \equiv M_D = Y_3 v_1 + Y_4 v_2. \tag{2.7}$$

In contrast to Yukawa couplings, which are complex, v_1 and v_2 are here assumed to be real. Typically, in the context of left-right symmetric theories, one investigates mainly the generation of Majorana neutrino masses. However, we note that when $v_2 \ll v_1$ and $|Y_3| \ll |Y_4|$ one can have small Dirac neutrino masses. In this scenario, the charged lepton and neutrino masses can be written as

$$M_e \approx Y_4 v_1, \tag{2.8}$$

$$M_D^\nu = v_1\left(Y_3 + M_e \frac{v_2}{|v_1|^2}\right). \tag{2.9}$$

The gauge couplings of $SU(2)_L, SU(2)_R$, and $U(1)_{B-L}$ are denoted as g_L, g_R, and g_{BL} respectively. When the gauge couplings of $SU(2)_L$ and $SU(2)_R$ gauge group become equal, i.e., $g_L = g_R$, there exist two symmetry transformations between the left and the right. This additional discrete left-right symmetry corresponds to either generalized parity $\mathcal{P}$ or generalized charge conjugation $\mathcal{C}$ [32,78]. Under the parity symmetry operation, the fields change as follows:

$$\begin{aligned} &\ell_L \overset{\mathcal{P}}{\leftrightarrow} \ell_R, \qquad q_L \overset{\mathcal{P}}{\leftrightarrow} q_R, \\ &\Phi \overset{\mathcal{P}}{\leftrightarrow} \Phi^\dagger, \qquad H_L \overset{\mathcal{P}}{\leftrightarrow} H_R, \qquad \tilde{\Phi} \overset{\mathcal{P}}{\leftrightarrow} \tilde{\Phi}^\dagger, \end{aligned} \tag{2.10}$$

whereas charge conjugation operation transforms the fields as

$$\begin{aligned} &\ell_L \overset{\mathcal{C}}{\leftrightarrow} \ell_R^c, \qquad q_L \overset{\mathcal{C}}{\leftrightarrow} q_R^c, \\ &\Phi \overset{\mathcal{C}}{\leftrightarrow} \Phi^T, \qquad H_L \overset{\mathcal{C}}{\leftrightarrow} H_R^*, \qquad \tilde{\Phi} \overset{\mathcal{C}}{\leftrightarrow} \tilde{\Phi}^T. \end{aligned} \tag{2.11}$$

All the left-right symmetric models either have a $\mathcal{P}$ or $\mathcal{C}$ symmetry. It should be noted that the combination of the two symmetries, $\mathcal{CP}$, does not switch the left and right-handed fields, and is not, therefore, a left-right symmetry. The Lagrangian in Eq. (2.4) becomes invariant by imposing left-right symmetry with discrete $\mathcal{P}$ symmetry and it leads to Hermitian Yukawa matrices as follows:

$$Y_1 = Y_1^\dagger, \qquad Y_2 = Y_2^\dagger, \qquad Y_3 = Y_3^\dagger, \qquad Y_4 = Y_4^\dagger. \tag{2.12}$$

Therefore quark, charged lepton and Dirac mass matrices presented in Eqs. (2.6) and (2.7) are Hermitian matrices. On the other hand, if discrete $\mathcal{C}$ symmetry is imposed on the Lagrangian in Eq. (2.4), it leads to symmetric Yukawa matrices,

$$Y_1 = Y_1^T, \qquad Y_2 = Y_2^T, \qquad Y_3 = Y_3^T, \qquad Y_4 = Y_4^T, \tag{2.13}$$

and the corresponding mass matrices of Eqs. (2.6) and (2.7) become symmetric matrices. However, in our discussion, we consider a left-right model with discrete $\mathcal{P}$ symmetry.

III. NEUTRINO MASSES AND MIXING

In order to implement the double (or cascade) seesaw mechanism [27,28] of neutrino mass generation within the manifest left-right symmetric model, we extend the fermion sector with the addition of one sterile neutrino $S_L \equiv [1,1,0]$ $\left(S_L \overset{\mathcal{P}}{\leftrightarrow} (S^c)_R\right)$ per generation. The relevant interaction Lagrangian $\mathcal{L}_{LRDSM}$ is given by

$$-\mathcal{L}_{LRDSM} = \mathcal{L}_{M_D} + \mathcal{L}_{M_{RS}} + \mathcal{L}_{M_S}, \tag{3.1}$$

where the individual terms can be expanded as follows:

(i) $\mathcal{L}_{M_D}$ is the Dirac mass term connecting left-handed and right-handed neutrino fields $\nu_L - N_R$:

$$\begin{aligned} \mathcal{L}_{M_D} &= \sum_{\alpha,\beta} \overline{\nu_{\alpha L}} [M_D]_{\alpha\beta} N_{\beta R} + \text{h.c.} \\ &\subset \sum_{\alpha,\beta} \overline{\ell_{\alpha L}} \left((Y_\ell)_{\alpha\beta}\Phi + (\tilde{Y}_\ell)_{\alpha\beta}\tilde{\Phi}\right)\ell_{\beta R} + \text{H.c.} \end{aligned} \tag{3.2}$$

(ii) $\mathcal{L}_{M_{RS}}$ is another Dirac mass term connecting N_R and S_L and in the considered left-right symmetric theory it has the form:

$$\begin{aligned} \mathcal{L}_{M_{RS}} &= \sum_{\alpha,\beta} \overline{S_{\alpha L}} [M_{RS}]_{\alpha\beta} N_{\beta R} + \text{H.c.} \\ &\subset \sum_{\alpha,\beta} \overline{S_{\alpha L}} (Y_{RS})_{\alpha\beta} \widetilde{H_R}^\dagger \ell_{\beta R} + \text{H.c.} \end{aligned} \tag{3.3}$$

(iii) The bare Majorana mass term $\mathcal{L}_{M_S}$ for sterile neutrinos S_L is given by

$$\begin{aligned} \mathcal{L}_{M_S} &= \frac{1}{2}\sum_{\alpha,\beta} \overline{S_{\alpha R}^c} [M_S]_{\alpha\beta} S_{\beta L} + \text{H.c.} \\ &\subset \sum_{\alpha,\beta} \frac{1}{2} (M_S)_{\alpha\beta} \overline{S_{\alpha R}^c} S_{\beta L} + \text{H.c.}, \end{aligned} \tag{3.4}$$

where $S_{\alpha R}^c \equiv C(\overline{S_{\alpha L}})^T$, C being the charge conjugation matrix ($C^{-1}\gamma_\mu C = -\gamma_\mu^T$). We have taken into account the scalar fields' VEVs as $\langle H_R^0 \rangle = v_R$ and $\langle H_L^0 \rangle = 0$, which prevents the mass term from linking $\nu_L - S_R^c$ through the interaction $\sum_{\alpha,\beta} \overline{\ell_{\alpha L}} (Y_{LS})_{\alpha\beta} \widetilde{H_L} S_{\beta R}^c + \text{h.c.}$ despite being permitted by gauge symmetry.

A. The double seesaw approximation

After the spontaneous symmetry breaking, the complete 9×9 neutral fermion mass matrix in the flavor basis of (ν_L, N_R^c, S_L) can be written as

$$\mathcal{M}_{LRDSM} = \begin{bmatrix} \mathbf{0} & M_D & \mathbf{0} \\ M_D^T & \mathbf{0} & M_{RS} \\ \mathbf{0} & M_{RS}^T & M_S \end{bmatrix}. \tag{3.5}$$

We assume in what follows that $|M_D| \ll |M_{RS}| \ll |M_s|$. This allows us to apply to the mass matrix $\mathcal{M}_{LRDSM}$ twice the seesaw approximate block diagonalization procedure for getting the mass matrices of light and heavy neutrinos, as discussed below.

1. First seesaw approximation

We implement the first seesaw block diagonalization procedure on the lower right 6×6 submatrix of $\mathcal{M}_{LRDSM}$ as indicated below

$$\mathcal{M}_{LRDSM} = \left[\begin{array}{c|cc} \mathbf{0} & M_D & \mathbf{0} \\ \hline M_D^T & 0 & M_{RS} \\ \mathbf{0} & M_{RS}^T & M_S \end{array}\right] \xrightarrow[\text{1st seesaw}]{M_S > M_{RS} \gg M_D} \left[\begin{array}{c|cc} \mathbf{0} & M_D & \mathbf{0} \\ \hline M_D^T & -M_{RS}M_S^{-1}M_{RS}^T & \mathbf{0} \\ \mathbf{0} & \mathbf{0} & M_S \end{array}\right]. \tag{3.6}$$

2. Second seesaw approximation

Denoting $-M_{RS}M_S^{-1}M_{RS}^T = M_R$, which is the expression for the mass matrix for right-handed neutrinos, we repeat the diagonalization procedure with seesaw condition, $|M_R| \gg |M_D|$. We get the resultant matrix structure as

$$\left[\begin{array}{cc|c} \mathbf{0} & M_D & \mathbf{0} \\ M_D^T & M_R & \mathbf{0} \\ \hline \mathbf{0} & \mathbf{0} & M_S \end{array}\right] \xrightarrow[\text{2nd seesaw}]{M_R \gg M_D} \left[\begin{array}{c|c|c} -M_D M_R^{-1} M_D^T & 0 & 0 \\ \hline 0 & M_R & 0 \\ \hline 0 & 0 & M_S \end{array}\right]. \tag{3.7}$$

Using the above results, the light neutrino, the heavy neutrino and sterile fermions mass matrices m_ν, m_N, and m_S can be expressed as

$$\begin{aligned} m_\nu &\cong -M_D(-M_{RS}M_S^{-1}M_{RS}^T)^{-1}M_D^T \\ &= \frac{M_D}{M_{RS}^T} M_S \frac{M_D^T}{M_{RS}}, \\ m_N &\equiv M_R \cong -M_{RS}M_S^{-1}M_{RS}^T, \\ m_S &\cong M_S. \end{aligned} \tag{3.8}$$

In the double seesaw expression for the light neutrino Majorana mass matrix as given in Eq. (3.8), different choices of M_D and M_{RS} are possible. Following [79–84], we have considered in the present article the case of M_D and M_{RS} being proportional to identity such that $M_D = k_d I$ and $M_{RS} = k_{rs} I$, where k_d and k_{rs} are real constants with $|k_d| < |k_{rs}|$. This means, $M_D M_{RS}^{-1} = \frac{k_d}{k_{rs}} I$. As discussed in [69,81], the equality and simultaneous diagonal structures of M_D and M_{RS} may arise as a consequence of $Z_2 \times Z_2$ symmetry [82]. With the introduction of additional permutation symmetry in the diagonal elements of M_D and M_{RS}, one can get equal diagonal elements. As we have indicated, these kinds of considerations have been reasoned for the double seesaw mechanism, e.g., in Refs. [79–84].

With the choices for the forms of M_D and M_{RS} made above, the relation between light neutrino and sterile neutrino mass matrices m_ν and m_S can be written as $m_\nu = \frac{k_d^2}{k_{rs}^2} m_S$. The mass matrix m_N can also be determined from Eq. (3.8) and the relationship between light neutrino and heavy right-handed neutrino mass matrices m_ν and m_N has the form $m_N = -k_d^2 \frac{1}{m_\nu}$.

In the basis in which the charged-lepton mass matrix is diagonal we will work within what follows. The light neutrino Majorana mass matrix is diagonalized with the help of a unitary mixing matrix—the Pontecorvo-Maki-Nakagawa-Sakata (PMNS) mixing matrix $U_{\text{PMNS}} \equiv U_\nu$ [85–87],

$$m_\nu^{\text{diag}} = U_{\text{PMNS}}^\dagger m_\nu U_{\text{PMNS}}^* = \text{diag}(m_1, m_2, m_3), \qquad m_i > 0,$$

so the physical masses m_i are related to the mass matrix m_ν in the flavor basis as

$$m_\nu = U_{\text{PMNS}} m_\nu^{\text{diag}} U_{\text{PMNS}}^T.$$

The right-handed neutrino Majorana mass matrix m_N is diagonalized as $\widehat{m_N} = {U_N}^\dagger m_N U_N^*$, $\widehat{m_N} = \text{diag}(m_{N_1}, m_{N_2}, m_{N_3})$, m_{N_j} being the mass of the heavy RH Majorana neutrino N_j, $j = 1, 2, 3$. It proves convenient to work with positive masses of N_j, $m_{N_j} > 0$. Given the relation $m_N = -k_d^2 \frac{1}{m_\nu}$ and the positivity of the eigenvalues of m_ν, the requirement that the eigenvalues of m_N are also positive implies that the unitary transformation matrices diagonalizing the light neutrino and the heavy right-handed neutrino mass matrices m_ν and m_N are related in the following way:

$$U_N = iU_\nu^* \equiv iU_{\rm PMNS}^*. \tag{3.9}$$

Since $m_S = (k_{rs}^2/k_d^2)m_\nu$, the diagonalization of the sterile-neutrino Majorana mass matrix m_S, $\widehat{m_S} = U_S{}^\dagger m_S U_S{}^*$, where $\widehat{m_S} = {\rm diag}(m_{S_1}, m_{S_2}, m_{S_3})$, $m_{S_k} > 0$, $k = 1, 2, 3$, can be performed with the help of the same mixing matrix $U_{\rm PMNS}$,

$$U_S = U_\nu \equiv U_{\rm PMNS}. \tag{3.10}$$

Thus, in the considered scenario, the light neutrino masses m_i, the heavy RH neutrino masses m_{N_j} and the sterile neutrino masses (m_{S_k}) are related as follows:

$$m_i = \frac{k_d^2}{m_{N_i}} = \frac{k_d^2}{k_{rs}^2} m_{S_i}, \quad i = 1, 2, 3. \tag{3.11}$$

In what follows, we will use the standard parametrization of the PMNS matrix (see, e.g., [88]):

$$U_{\rm PMNS} = \begin{pmatrix} c_{13}c_{12} & c_{13}s_{12} & s_{13}e^{-i\delta} \\ -c_{23}s_{12} - c_{12}s_{13}s_{23}e^{i\delta} & c_{12}c_{23} - s_{12}s_{13}s_{23}e^{i\delta} & s_{23}c_{13} \\ s_{12}s_{23} - c_{12}c_{23}s_{13}e^{i\delta} & -c_{12}s_{23} - s_{12}s_{13}c_{23}e^{i\delta} & c_{13}c_{23} \end{pmatrix} {\rm P} \tag{3.12}$$

where the mixing angles are denoted by $s_{ij} = \sin\theta_{ij}$, $c_{ij} = \cos\theta_{ij}$, $0 \le \theta_{ij} \le \pi/2$, δ is the Dirac CP violation phase, $0 \le \delta \le 2\pi$, P is the diagonal phase matrix containing the two Majorana CP violation phases α and β [89], ${\rm P} = {\rm diag}(1, e^{i\alpha/2}, e^{i\beta/2})$. The Majorana phases take values in the interval $[0, \pi]$. The experimental values of different oscillation parameters for the light neutrino mass spectrum with normal ordering (NO) and inverted ordering (IO) (see, e.g., [88]) are taken from Ref. [90] and are presented in Table II.

3. Masses of light neutrinos

It proves convenient to express the masses of the two heavier neutrinos in terms of the lightest neutrino mass and the neutrino mass squared differences measured in neutrino oscillation experiments. In the case of NO light neutrino mass spectrum, $m_1 < m_2 < m_3$, we have:

$$\begin{aligned} m_1 &= \text{lightest neutrino mass}, \\ m_2 &= \sqrt{m_1^2 + \Delta m_{\rm sol}^2}, \\ m_3 &= \sqrt{m_1^2 + \Delta m_{\rm atm}^2}, \end{aligned} \tag{3.13}$$

where $\Delta m_{\rm sol}^2 = \Delta m_{21}^2$ and $\Delta m_{\rm atm}^2 = \Delta m_{31}^2$. Similarly, for inverted mass ordering, $m_3 < m_1 < m_2$, we get

$$\begin{aligned} m_3 &= \text{lightest neutrino mass}, \\ m_1 &= \sqrt{m_3^2 - \Delta m_{\rm sol}^2 - \Delta m_{\rm atm}^2}, \\ m_2 &= \sqrt{m_3^2 - \Delta m_{\rm atm}^2}, \end{aligned} \tag{3.14}$$

with $\Delta m_{\rm sol}^2 = \Delta m_{21}^2$ and $\Delta m_{\rm atm}^2 = \Delta m_{32}^2$.

Depending on the value of the lightest neutrino mass the neutrino mass spectrum can also be normal hierarchical (NH) when $m_1 \ll m_2 < m_3$, inverted hierarchical (IH) if $m_3 \ll m_1 < m_2$, or else quasidegenerate (QD) when $m_1 \cong m_2 \cong m_3$, $m_{1,2,3}^2 \gg \Delta m_{31(23)}^2$, i.e., $m_{1,2,3} \gtrsim 0.1$ eV.

All considered types of neutrino mass spectrum are compatible with the existing data. The best upper limit on the lightest neutrino mass $m_{1(3)}$ has been obtained in the KATRIN experiment. It is in the range of the QD spectrum and effectively reads: $m_{1,2,3} < 0.80$ eV (90% C.L.).

4. Masses of heavy RH neutrinos

Since m_i and m_{N_j} are inversely proportional to each other, for NO light neutrino mass spectrum, $m_1 < m_2 < m_3$, m_{N_1} has to be the largest RH neutrino mass. We can express m_{N_2} and m_{N_3} in terms of m_{N_1} and the light neutrino masses,

$$m_{N_2} = \frac{m_1}{m_2} m_{N_1}, \qquad m_{N_3} = \frac{m_1}{m_3} m_{N_1}, \qquad m_{N_3} < m_{N_2} < m_{N_1}. \tag{3.15}$$

In the case of IO spectrum, $m_3 < m_1 < m_2$, m_{N_3} is the largest mass. The mass relations in this case become

$$m_{N_1} = \frac{m_3}{m_1} m_{N_3}, \qquad m_{N_2} = \frac{m_3}{m_2} m_{N_3}, \qquad m_{N_1} < m_{N_2} < m_{N_3}. \tag{3.16}$$

5. Masses of sterile neutrinos

Since m_i and m_{S_k} are directly proportional to each other; in the NO case m_{S_3} is the heaviest sterile neutrino mass and the analogous mass relations read

$$m_{S_1} = \frac{m_1}{m_3} m_{S_3}, \qquad m_{S_2} = \frac{m_2}{m_3} m_{S_3}, \qquad m_{S_1} < m_{S_2} < m_{S_3}. \tag{3.17}$$

For the IO spectrum we have $m_{S_3} < m_{S_1} < m_{S_2}$ and

$$m_{S_1} = \frac{m_1}{m_2} m_{S_2}, \qquad m_{S_3} = \frac{m_3}{m_2} m_{S_2}, \qquad m_{S_3} < m_{S_1} < m_{S_2}. \tag{3.18}$$

6. Neutrino mixing

The diagonalization of $\mathcal{M}_{\rm LRDSM}$ leads to the following relation between the fields of the neutral fermions written in the flavor (weak interaction eigenstate) basis and in the mass eigenstate basis,

$$\begin{pmatrix} \nu_{\alpha L} \\ N^c_{\beta L} \\ S_{\gamma L} \end{pmatrix} = \begin{pmatrix} V^{\nu\nu}_{\alpha i} & V^{\nu N}_{\alpha j} & V^{\nu S}_{\alpha k} \\ V^{N\nu}_{\beta i} & V^{NN}_{\beta j} & V^{NS}_{\beta k} \\ V^{S\nu}_{\gamma i} & V^{SN}_{\gamma j} & V^{SS}_{\gamma k} \end{pmatrix} \begin{pmatrix} \nu_{iL} \\ N^c_{jL} \\ S_{kL} \end{pmatrix}. \tag{3.19}$$

Here $N^c_{\beta L} \equiv C(\overline{N_{\beta R}})^T$, $N^c_{jL} \equiv C(\overline{N_{jR}})^T = N_{jL}$ (N_j are Majorana fields), C being the charge-conjugation matrix, the indices α, β, γ run over three generations of light left-handed neutrinos, heavy right-handed neutrinos and sterile neutrinos in flavor basis respectively, whereas the indices i, j, k, run over corresponding mass eigenstates. The mixing matrix elements in Eq. (3.19) are given in Eq. (A27) in the Appendix. The mixing between the right-handed neutrinos and sterile neutrinos $(N^c_L - S_L)$ is given by the term,

$$V^{NS} \propto M_{RS} M_S^{-1} \tag{3.20}$$

while the mixing between the fields of the left-handed flavor neutrinos and the heavy right-handed neutrinos $(\nu_L - N^c_L)$ is determined by

$$V^{\nu N} \propto M_D M_R^{-1} = -M_D M_{RS}^{T\,-1} M_S M_{RS}^{-1} \tag{3.21}$$

The mixing between sterile and light neutrinos $(\nu_L - S_L)$ is vanishing, $V^{\nu S}_{\alpha k} \cong 0$ and $V^{S\nu}_{\gamma i} \cong 0$.

The possible sets of numerical values for different mixing matrices, masses and mixing that can give rise to dominant contributions to LNV decays are listed in Table I. By choosing one representative set of model parameters from the table, we get the mixing as given below,

TABLE I. A representative set of model parameters in left-right symmetric models and the order of magnitude estimation of various neutrino masses within the double seesaw mechanism. All the masses are expressed in units of GeV except the light neutrino masses, which are in the eV scale.

M_D	M_{RS}	M_S	m_ν (eV)	m_N	m_S	$V^{\nu N}$	V^{NS}
10^{-4}	10^3	10^4	0.1	10^2	10^4	10^{-6}	0.1
10^{-5}	10^2	10^3	0.01	10	10^3	10^{-6}	0.1
10^{-5}	10^1	10^2	0.1	1	10^2	10^{-5}	0.1

$$\begin{pmatrix} V^{\nu\nu}_{\alpha i} & V^{\nu N}_{\alpha j} & V^{\nu S}_{\alpha k} \\ V^{N\nu}_{\beta i} & V^{NN}_{\beta j} & V^{NS}_{\beta k} \\ V^{S\nu}_{\gamma i} & V^{SN}_{\gamma j} & V^{SS}_{\gamma k} \end{pmatrix} \simeq \begin{pmatrix} \mathcal{O}(1.0) & \mathcal{O}(10^{-6}) & 0 \\ \mathcal{O}(10^{-6}) & \mathcal{O}(1.0) & \mathcal{O}(0.1) \\ 0 & \mathcal{O}(0.1) & \mathcal{O}(1.0) \end{pmatrix}. \tag{3.22}$$

In the above matrix, the nonzero elements come from $V^{\nu\nu}_{\alpha i}$, $V^{NN}_{\beta j}$, $V^{NS}_{\beta k}$, $V^{SN}_{\gamma j}$, and $V^{SS}_{\gamma k}$ while all other terms are negligibly small. These nonzero mixings would contribute sizeably to the predicted neutrinoless double beta decay rate. Thus, Eq. (3.19) can be rewritten for the fields of flavor neutrinos $\nu_{\alpha L}$ and the heavy RH neutrinos $N^c_{\beta L}$ as

$$\begin{aligned} \nu_{\alpha L} &\cong V^{\nu\nu}_{\alpha i} \nu_{iL} + V^{\nu N}_{\alpha j} N_{jL}, \\ N^c_{\beta L} &= V^{N\nu}_{\beta i} \nu_{iL} + V^{NN}_{\beta j} N_{jL} + V^{NS}_{\beta k} S_{kL}. \end{aligned} \tag{3.23}$$

As we have indicated, in the considered model we have $|V^{\nu N}_{\alpha j}| \sim 10^{-6}$. Correspondingly, the contribution to the $0\nu\beta\beta$ decay amplitude arising from the coupling of N_{jL} to the electron in the LH (i.e., V-A) charged lepton current involves the factor $(V^{\nu N}_{ej})^2$ and is negligible.

B. Gauge boson masses

We briefly summarize here the gauge bosons masses and mixing in our model which will be used in estimating half-life of neutrinoless double beta decay process. Besides the SM gauge bosons $W^\pm_L$ and Z, there are right-handed gauge bosons $W^\pm_R$ and Z' which get their masses from left-right symmetry breaking. Following Ref. [32] and choosing VEVs of the Higgs fields as

$$\langle H^0_R \rangle = v_R, \qquad \langle \phi^0_{1,2} \rangle = v_{1,2}, \tag{3.24}$$

the mass matrix for charged gauge bosons, in the basis $(W^+_L W^+_R)$ can be written as

$$\mathbb{M}_{CGB} = \begin{pmatrix} \frac{g_L^2 v^2}{2} & -g_L g_R v_1 v_2 \\ -g_L g_R v_1 v_2 & \frac{g_R^2}{2}\left(\frac{1}{2} v_R^2 + v^2\right) \end{pmatrix},$$

where $v^2 = v_1^2 + v_2^2$ and $g_R = g_L$. The physical mass for extra charged gauge boson is given by

$$M_{W_R} \simeq \frac{1}{2} g_R v_R. \tag{3.25}$$

The mixing angle between W_R and W_L is defined as

$$\tan 2\theta_{LR} \approx 8\frac{g_L}{g_R}\frac{v_1 v_2}{v_R^2}.$$

The neutral gauge boson mass matrix is given by

$$\mathbb{M}_{NGB} = \begin{pmatrix} \frac{g_L^2 v^2}{2} & -\frac{g_L g_R}{2} v^2 & 0 \\ -\frac{g_L g_R}{2} v^2 & \frac{g_R^2}{2}\left(\frac{1}{2}v_R^2 + v^2\right) & -\frac{g_R g_{BL}}{4} v_R^2 \\ 0 & -\frac{g_R g_{BL}}{4} v_R^2 & \frac{g_{BL}^2 v_R^2}{4} \end{pmatrix}.$$

As can be easily checked, this mass matrix has one zero eigenvalue corresponding to the photon A_μ. After few simplification, the mass eigenstates Z_μ, Z'_μ, and A_μ are related to the weak eigenstates $(W^0_{L\mu}, W^0_{R\mu}, Z_{BL\mu})$ in the following way:

$$\begin{aligned} W^0_{L\mu} &= \cos\theta_W Z_{L\mu} + \sin\theta_W A_\mu, \\ W^0_{R\mu} &= \cos\theta_R Z_{R\mu} - \sin\theta_W \sin\theta_R Z_{L\mu} + \cos\theta_W \sin\theta_R A_\mu, \\ Z^0_{BL\mu} &= -\sin\theta_R Z_{R\mu} - \sin\theta_W \cos\theta_R Z_{L\mu} + \cos\theta_W \cos\theta_R A_\mu, \end{aligned}$$

where

$$\begin{aligned} Z_{L\mu} &\equiv Z_\mu \cos\xi + Z'_\mu \sin\xi, \\ Z_{R\mu} &\equiv -Z_\mu \sin\xi + Z'_\mu \cos\xi. \end{aligned} \tag{3.26}$$

Here, the mixing angles are defined as $\tan\theta_R = g_{BL}/g_R$, $\tan\theta_W = g_Y/g_L$ with $g_Y = g_{BL}g_R/\sqrt{g_{BL}^2 + g_R^2}$, while the mixing angle between the Z and the heavy Z' reads,

$$\tan 2\xi \approx \frac{v_1 v_2}{v_R^2}\frac{-4g_R^2\sqrt{g_L^2 g_R^2 + g_{BL}^2(g_L^2 + g_R^2)}}{(g_{BL}^2 + g_R^2)^2}. \tag{3.27}$$

The physical mass for extra neutral gauge boson Z' is given by

$$M_{Z'}^2 \simeq \frac{1}{2}(g_{BL}^2 + g_R^2)\left[v_R^2 + \frac{g_R^2 v^2}{g_R^2 + g_{BL}^2}\right]. \tag{3.28}$$

The value of $\tan 2\xi$ has to be smaller than 10^{-3} in order to satisfy the electroweak precision constraints in the limit $v_R^2 \gg v_1^2 + v_2^2$. With $v^2 = v_1^2 + v_2^2 \simeq (246\ \text{GeV})^2$ and $g_R \simeq g_L = 0.653$, we have $\tan\theta_W = \frac{g_{BL}}{\sqrt{g_{BL}^2+g_R^2}}$, which implies $\frac{g_{BL}^2}{g_{L/R}^2} = \frac{\sin^2\theta_W}{1-2\sin^2\theta_W} \approx 0.43$, where $\sin^2\theta_W = 0.231$. Using this result and $g_L = g_R$, we get for the angle describing the $Z - Z'$ mixing: $|\tan 2\xi| \cong 2.67 v_1 v_2/v_R^2$. The upper limit $|\tan 2\xi| < 10^{-3}$ implies

$$\frac{v_1 v_2}{v_R^2} < 3.75 \times 10^{-4}. \tag{3.29}$$

TABLE II. The current updated estimates of experimental values of neutrino oscillation parameters for global best fits and 3σ range taken from [90].

Parameter	Best-fit values	3σ range
$\Delta m_{21}^2[10^{-5}\ \text{eV}]$	7.34	6.92–7.90
$\lvert\Delta m_{31}^2\rvert[10^{-3}\ \text{eV}]$ (NO)	2.485	2.389–2.578
$\lvert\Delta m_{32}^2\rvert[10^{-3}\ \text{eV}]$ (IO)	2.465	2.374–2.556
$\sin^2\theta_{12}/10^{-1}$ (NO)	3.05	2.65–3.47
$\sin^2\theta_{12}/10^{-1}$ (IO)	3.03	2.64–3.45
$\sin^2\theta_{23}/10^{-1}$ (NO)	5.45	4.36–5.95
$\sin^2\theta_{23}/10^{-1}$ (I)	5.51	4.39–5.96
$\sin^2\theta_{13}/10^{-2}$ (NO)	2.22	2.01–2.41
$\sin^2\theta_{13}/10^{-2}$ (IO)	2.23	2.03–2.43

This in turn leads to the following upper limit on the $W_L - W_R$ mixing angle θ_{LR}:

$$\theta_{LR} \cong 4\frac{v_1 v_2}{v_R^2} < 1.50 \times 10^{-3}. \tag{3.30}$$

The left-handed gauge boson masses are similar to those of the SM gauge bosons with $g_Y = (g_R g_{BL})/(g_R^2 + g_{BL}^2)^{1/2}$, while the masses of the extra heavy gauge bosons are related as follows:

$$M_{W_R} \simeq \frac{1}{2} g_R v_R, \tag{3.31}$$

$$M_{Z'} \simeq \frac{\sqrt{g_{BL}^2 + g_R^2}}{g_R} M_{W_R} \simeq 1.2 M_{W_R}. \tag{3.32}$$

The current experimental bound on $M_{W_R} > 5$ TeV is obtained in high-energy collider experiments at LHC [91–93], while the low-energy precision measurements [94,95] imply a lower bound on the Z' mass, i.e., $M_{Z'} > 6$ TeV.

IV. NEUTRINOLESS DOUBLE BETA DECAY

Neutrinoless double beta decay process can be induced by the exchange of light active Majorana neutrinos, which is usually referred to as "the standard mechanism," or by some other lepton number violating "nonstandard mechanism" associated with BSM physics. In this section, we discuss the standard and the new physics contributions to $0\nu\beta\beta$ decay amplitude and rate that arise in our model due to the exchange of the light Majorana neutrinos ν_i, heavy Majorana neutrinos $N_{1,2,3}$ and sterile Majorana neutrinos $S_{1,2,3}$.

The charged-current (CC) interaction Lagrangian for leptons and quarks, relevant for our further discussion, are given by

$$\mathcal{L}_{\rm CC}^{\ell} = \sum_{\alpha=e,\mu,\tau}\left[\frac{g_L}{\sqrt{2}}\overline{\ell}_{\alpha L}\gamma_\mu \nu_{\alpha L} W_L^\mu + \frac{g_R}{\sqrt{2}}\overline{\ell}_{\alpha R}\gamma_\mu N_{\alpha R} W_R^\mu\right] + \text{H.c.}$$
$$= \frac{g_L}{\sqrt{2}}\bar{e}_L\gamma_\mu \nu_{eL} W_L^\mu + \frac{g_R}{\sqrt{2}}\bar{e}_R\gamma_\mu N_{eR} W_R^\mu + \text{H.c.} + \cdots \tag{4.1}$$

$$\mathcal{L}_{\rm CC}^{\rm q} = \left[\frac{g_L}{\sqrt{2}}\bar{u}_L\gamma_\mu d_L W_L^\mu + \frac{g_R}{\sqrt{2}}\bar{u}_R\gamma_\mu d_R W_R^\mu\right] + \text{H.c.} \tag{4.2}$$

Using Eq. (3.23), $\mathcal{L}_{\rm CC}^{\ell}$ be rewritten as

$$\mathcal{L}_{\rm CC}^{\ell} = \frac{g_L}{\sqrt{2}}[\bar{e}_L\gamma_\mu\{\mathrm{V}_{ei}^{\nu\nu}\nu_i + \mathrm{V}_{ei}^{\nu N}N_i\}W_L^\mu] + \text{H.c.}$$
$$+ \frac{g_R}{\sqrt{2}}[\bar{e}_R\gamma_\mu\{\mathrm{V}_{ei}^{N\nu}\nu_i + \mathrm{V}_{ei}^{NN}N_i + \mathrm{V}_{ei}^{NS}S_i\}W_R^\mu] + \text{H.c.} \tag{4.3}$$

In the present model, the heavy neutrino masses are around 1–1000 GeV, $\nu_L - N_L^c$ mixing $|V_{\nu N}| \leq 10^{-6}$ and $\nu_L - S_L$ mixing is vanishing. Other contributions involving the light-heavy neutrino mixings and the $W_L - W_R$ mixing are negligible. The lepton Lagrangian that is relevant for the dominant contributions to $0\nu\beta\beta$ decay rate is

$$\mathcal{L}_{\rm CC}^{\ell} = \frac{g_L}{\sqrt{2}}[\bar{e}_L\gamma_\mu\{\mathrm{V}_{ei}^{\nu\nu}\nu_i\}W_L^\mu] + \text{H.c.}$$
$$+ \frac{g_R}{\sqrt{2}}[\bar{e}_R\gamma_\mu\{\mathrm{V}_{ej}^{NN}N_j + \mathrm{V}_{ek}^{NS}S_k\}W_R^\mu] + \text{H.c.} \tag{4.4}$$

Thus, in the considered model, the dominant contributions to the $0\nu\beta\beta$ decay amplitude are given by

(i) the standard mechanism due to the exchange of light neutrino ν_i, mediated by left-handed gauge boson W_L, i.e., due to purely left-handed (LH) CC interaction; and

(ii) new contributions due to the exchange of heavy neutrinos $N_{1,2,3}$ and sterile neutrinos $S_{1,2,3}$, mediated by right-handed gauge boson W_R, i.e., due to purely right-handed (RH) CC interaction. The contribution due to exchange of virtual $S_{1,2,3}$ is possible due to the mixing between N_L^c and S_L.

The so-called $\langle\lambda\rangle$- and $\langle\eta\rangle$- mechanism contributions $0\nu\beta\beta$ decay amplitude arising from the product of LH and RH lepton currents [96] are subdominant being strongly suppressed. The $\langle\lambda\rangle$-mechanism contribution involves the factor $|V_{ei}^{N\nu}|(M_{W_L}/M_{W_R})^2 < 2.6\times10^{-10}$, where we have used $|V_{ei}^{N\nu}| = 10^{-6}$, $M_{W_L} = 80.38$ GeV and $M_{W_R} > 5$ TeV, while the $\langle\eta\rangle$-mechanism contribution is suppressed by the factor $|V_{ei}^{N\nu}\sin\theta_{LR}| < 10^{-9}$. As a consequence, we neglect these contributions in the analysis which follows.

The Feynman diagrams for the dominant contributions of interest to the $0\nu\beta\beta$ decay amplitude are shown in Fig. 1, where the first diagram from the left corresponds to the standard mechanism, while the second and third diagrams correspond to the new contributions mediated by $N_{1,2,3}$ and $S_{1,2,3}$, respectively.

When $0\nu\beta\beta$ decay is mediated by only light Majorana neutrinos ν_i, the inverse half-life for this process can be expressed as

$$[T_{1/2}^{0\nu}]^{-1} = g_{\rm A}^4 G_{01}^{0\nu}|\mathcal{M}_\nu^{0\nu}|^2|\eta_\nu|^2, \tag{4.5}$$

where $g_{\rm A}$ is the axial coupling constant, $G_{01}^{0\nu}$ is the phase-space factor, $\mathcal{M}_\nu^{0\nu}$ are the nuclear matrix elements (NME) for light neutrino exchange and η_ν is a dimensionless particle physics parameter that is a measure of lepton number violation. Considering both the standard mechanism and the new contributions to this decay process in our model, the inverse half-life can be written as

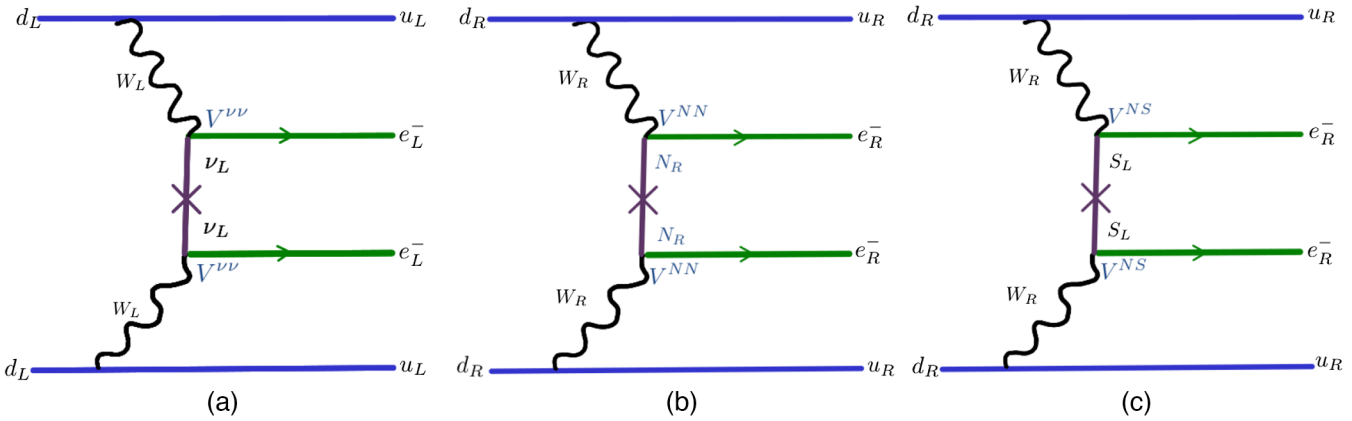

FIG. 1. Feynman diagrams for the process of neutrinoless double beta decay mediated by the exchane of virtual (a) light Majorana neutrinos ν_i (the standard mechanism), (b) heavy neutrinos N_R (heavy Majorana neutrinos $N_{1,2,3}$), and (c) heavy sterile neutrinos S_L (heavy Majorana neutrinos $S_{1,2,3}$).

$$[T^{0\nu}_{1/2}]^{-1} = g_A^4 G^{0\nu}_{01}[|\mathcal{M}^{0\nu}_{\nu}\cdot\eta_\nu|^2 + |\mathcal{M}^{0\nu}_{N}\cdot(\eta_N+\eta_S)|^2], \quad (4.6)$$

where $\mathcal{M}^{0\nu}_{N}$ are the nuclear matrix elements (NME) for the heavy neutrino exchange and η_N and η_S are lepton-number violating parameters associated with the exchange of the heavy neutrinos $N_{1,2,3}$ and $S_{1,2,3}$.

In the analysis and the numerical estimates which follow, we will use a mildly quenched value of the axial coupling constant $g_A = 1.00$, the unquenched value being, as is well known, $g_A = 1.27$. If it turns out that g_A is actually not quenched, that will reduce the estimates of the $0\nu\beta\beta$ decay half-lives made in the present study by a factor of 2.60.

The interference term of the light neutrino $\nu_{1,2,3}$ and the heavy neutrinos $N_{1,2,3}$ and $S_{1,2,3}$ exchange contributions to the $0\nu\beta\beta$ decay amplitude, which are generated respectively by LH $(V-A)$ CC and RH $(V+A)$ CC interactions, is strongly suppressed, being proportional to the electron mass [97] (see also [98]) and we have neglected it in Eq. (4.6).

The values of $G^{0\nu}_{01}$ and the NMEs for both light- and heavy-neutrino exchange mechanism are distinct for different isotopes and can be found, e.g., in [99]. We present in Table III the values obtained by six different groups of authors using different methods of NME calculation. Of particular importance for the estimates of the relative magnitude of the new nonstandard contributions in the $0\nu\beta\beta$ decay amplitude with respect to the contribution of the standard mechanism is the ratio $\mathcal{M}^{0\nu}_{N}/\mathcal{M}^{0\nu}_{\nu}$. As it follows from Table III, the ratio $\mathcal{M}^{0\nu}_{N}/\mathcal{M}^{0\nu}_{\nu}$ predicted by each of the six cited groups using different methods of NME calculation is essentially the same for the four isotopes ^{76}Ge, ^{82}Se, ^{130}Te, ^{136}Xe—it varies with the isotope by not more than ∼15%. At the same time, for a given isotope the ratio of interest obtained by the six different methods of NME calculation quoted in Table III varies by a factor of up to ∼3.5. In view of this we will use the values of the NMEs for ^{76}Ge as reference values in our numerical analysis. For the minimal and maximal values of the ratio $\mathcal{M}^{0\nu}_{N}/\mathcal{M}^{0\nu}_{\nu}$ for ^{76}Ge we get from Table III,

$$22.2 \lesssim \frac{\mathcal{M}^{0\nu}_{N}}{\mathcal{M}^{0\nu}_{\nu}} \lesssim 76.3, \qquad ^{76}\text{Ge}. \quad (4.7)$$

They correspond respectively to $\mathcal{M}^{0\nu}_{\nu} = 4.68$ and 5.26.

The dimensionless particle physics parameters η_ν, η_N, and η_s in Eq. (4.6) are functions of neutrino masses, mixing parameters and CPV phases and can be expressed as

$$|\eta_\nu| = \sum_{i=1,2,3} \frac{\mathrm{V}^{\nu\nu 2}_{ei} m_{\nu_i}}{m_e}, \quad (4.8)$$

$$|\eta_N| = m_p \left(\frac{M_{W_L}}{M_{W_R}}\right)^4 \sum_{j=1,2,3} \frac{\mathrm{V}^{NN2}_{ej}}{m_{N_j}}, \quad (4.9)$$

$$|\eta_S| = m_p \left(\frac{M_{W_L}}{M_{W_R}}\right)^4 \sum_{k=1,2,3} \frac{\mathrm{V}^{NS2}_{ek}}{m_{S_k}}, \quad (4.10)$$

where m_e and m_p are the electron and proton masses. The quantity $m_e|\eta_\nu| \equiv |m^{\nu}_{\beta\beta,L}|$ is the effective Majorana mass (EMM) associated with the standard mechanism of $0\nu\beta\beta$ decay (see, e.g., [18,110]).

In [111] it was noticed that there exists a short distance (contact) contribution to the $0\nu\beta\beta$ decay amplitude even in the case of light neutrino exchange. The magnitude of this contribution was investigated in a number of studies. Using the results of the estimates of the $nn \to ppee$ amplitude derived in [112] the magnitude of this contribution relative to the standard light neutrino exchange one was calculated for the neutrinoless double beta decay of ^{48}Ca in [113] and for ^{76}Ge, ^{130}Te, and ^{136}Xe in [114]. Both groups of authors find a positive contribution enhancing the standard one by about 43% and 30% respectively for ^{48}Ca and ^{76}Ge, ^{130}Te, ^{136}Xe. These effects are accounted for in our analysis by the much larger uncertainties in the NMEs included in the analysis.

The mixing parameters in Eqs. (4.8)–(4.10) are given in the Appendix. In the framework of our model we have $V^{\nu\nu} \approx U_\nu$, $V^{NN} \approx U_N$, and $V^{NS} \equiv M_{RS}M_S^{-1}U_S$. We recall

TABLE III. Values of nuclear matrix elements for various isotopes calculated by different methods for light and heavy neutrino exchange. Here QRPA-Jy uses CD-Bonn short range correlations (SRC) and the rest use Argonne SRC, with minimally quenched $g_A = 1$. The last row shows the phase space factor $G^{0\nu}_{01}$ for various isotopes [99,100].

	^{76}Ge		^{82}Se		^{130}Te		^{136}Xe	
Methods	$\mathcal{M}^{0\nu}_{\nu}$	$\mathcal{M}^{0\nu}_{N}$	$\mathcal{M}^{0\nu}_{\nu}$	$\mathcal{M}^{0\nu}_{N}$	$\mathcal{M}^{0\nu}_{\nu}$	$\mathcal{M}^{0\nu}_{N}$	$\mathcal{M}^{0\nu}_{\nu}$	$\mathcal{M}^{0\nu}_{N}$
dQRPA [101]	3.12	187.3	2.86	175.9	2.90	191.4	1.11	66.9
QRPA-Tu [102,103]	5.16	287.0	4.64	262.0	3.89	264.0	2.18	152.0
QRPA-Jy [104]	5.26	401.3	3.73	287.1	4.00	338.3	2.91	186.3
IBM-2 [105]	4.68	104	3.73	82.9	3.70	91.8	3.05	72.6
CDFT [106–108]	6.04	209.1	5.30	189.3	4.89	193.8	4.24	166.3
ISM [109]	2.89	130	2.73	121	2.76	146	2.28	116
$G^{0\nu}_{01}$ [10^{-14} yrs^{-1}] [100]	0.22		1		1.4		1.5	

that $U_N = iU_\nu^*$, $U_S = U_\nu$ and $U_\nu \equiv U_{\rm PMNS}$ [Eqs. (3.9) and (3.10)].

The expressions for $|\eta_N|$ and $|\eta_S|$ in Eqs. (4.9) and (4.10) are obtained under the condition $\langle p^2\rangle \ll M_i^2$, where $\sqrt{\langle p^2\rangle}$ is the average momentum exchanged in the process of $0\nu\beta\beta$ decay and M_i here is a generic notation for the masses of $N_{1,2,3}$ and $S_{1,2,3}$. The chiral structure of the matrix elements involving virtual $N_{1,2,3}$ and $S_{1,2,3}$ propagators in the case of the heavy-neutrino exchange contribution is given by

$$P_R \frac{\not{p} + M_i}{p^2 - M_i^2} P_R = \frac{M_i}{p^2 - M_i^2} P_R, \tag{4.11}$$

where $P_R = (1+\gamma_5)/2$ is the RH projection operator. A typical value of the neutrino virtuality is $\langle p^2\rangle \cong (190\ \text{MeV})^2$ (see, e.g., [115]). Thus, in the case of interest, we have $p^2 \ll M_i^2$ and the heavy-state propagators reduce to a good approximation to $1/M_i$.

It proves convenient for our further analysis to rewrite the inverse half-life in terms of one particle-physics parameter—generalized effective Majorana mass (GEMM)—that contains the lepton-number violating information in it,

$$\begin{aligned}[T^{0\nu}_{1/2}]^{-1} &= G^{0\nu}_{01}[|\mathcal{M}^{0\nu}_\nu \eta_\nu|^2 + \mathcal{M}^{0\nu}_N|\eta_N + \eta_S|^2] \\ &= G^{0\nu}_{01}\left|\frac{\mathcal{M}^{0\nu}_\nu}{m_e}\right|^2 [|m^\nu_{\beta\beta,L}|^2 + |m^N_{\beta\beta,R} + m^S_{\beta\beta,R}|^2] \\ &= G^{0\nu}_{01}\left|\frac{\mathcal{M}^{0\nu}_\nu}{m_e}\right|^2 |m^{\rm eff}_{\beta\beta,L,R}|^2, \end{aligned} \tag{4.12}$$

where [115]

$$\begin{aligned} m^N_{\beta\beta,R} &= \sum_j m_p m_e \frac{\mathcal{M}^{0\nu}_N}{\mathcal{M}^{0\nu}_\nu}\frac{M^4_{W_L}}{M^4_{W_R}}\frac{\mathrm{V}^{NN2}_{ej}}{m_{N_j}}, \\ m^S_{\beta\beta,R} &= \sum_k m_p m_e \frac{\mathcal{M}^{0\nu}_N}{\mathcal{M}^{0\nu}_\nu}\frac{M^4_{W_L}}{M^4_{W_R}}\frac{\mathrm{V}^{NS2}_{ek}}{m_{S_k}}. \end{aligned} \tag{4.13}$$

It follows from Eqs. (4.9), (4.10), and (4.13) that the new physics contributions to the $0\nu\beta\beta$ decay amplitude are suppressed, in particular, by the factor $M^4_{W_L}/M^4_{W_R} < (1.6\times 10^{-2})^4$, where $M_{W_L} = 80.38$ GeV is the SM W-bosons mass and we have used the lower bound $M_{W_R} > 5$ TeV [91–95]. Fixing M_{W_R} at, e.g., $= 5.5$ TeV, we have for the ratio $(M^4_{W_L}/M^4_{W_R}) \sim \mathcal{O}(10^{-8})$. Taking further the masses of S_k and N_j in the ranges respectively of $(10^2$–$10^4)$ GeV and $(1$–$10^2)$ GeV, the mixing $V^{NN}_{ej} \approx U_N$ and $V^{NS}_{ek} \equiv M_{RS}M_S^{-1}U_S$ from the Appendix, one finds that the new physics contributions can be in the 0.01–0.1 eV range (see Table IV), i.e., within the experimental search sensitivity.

We note that, since the dominant contributions to $0\nu\beta\beta$ decay arises from more than one contribution, it is also possible that there might be interference between them in the decay rate of the process. The interference of light neutrino (ν_i) contribution due to purely $V-A$ interaction involving LH currents with either of the heavy-neutrino N_j and S_k contributions, which are generated by $(V+A)$ interaction with RH currents, is suppressed, as we have indicated earlier. However, the interference between the contributions of the heavy neutrinos N_j and S_k both involving RH currents, in general, cannot be neglected. In the case when this interference is not taken into consideration, the generalized effective Majorana mass is determined by the sum of individual contributions of the three types of neutrinos ν_i, N_j, and S_k,

$$|m^{\rm eff}_{\beta\beta,L,R}| \equiv m^{\nu+N+S}_{ee} = (|m^\nu_{\beta\beta,L}|^2 + |m^N_{\beta\beta,R}|^2 + |m^S_{\beta\beta,R}|^2)^{\frac{1}{2}}. \tag{4.14}$$

Accounting for the interference, the generalized effective Majorana mass can be written as

$$\begin{aligned} |m^{\rm eff}_{\beta\beta,L,R}| \equiv m^{\nu+|N+S|}_{ee} &= (|m^\nu_{\beta\beta,L}|^2 + |m^N_{\beta\beta,R} + m^S_{\beta\beta,R}|^2)^{\frac{1}{2}} \\ &= ((m^{\nu+N+S}_{ee})^2 + 2\mathrm{Re}(m^N_{\beta\beta,R}\cdot m^{S^*}_{\beta\beta,R}))^{\frac{1}{2}}. \end{aligned} \tag{4.15}$$

TABLE IV. The current lower limits on the half-life $T^{0\nu}_{1/2}$ and upper limits on the effective mass parameter $m^{0\nu}_{\beta\beta}$ of neutrinoless double beta decay for different isotopes. The range for the effective Majorana mass parameter comes from uncertainties in the nuclear matrix element.

Isotope	$T^{0\nu}_{1/2}$ yrs	$m^{0\nu}_{\beta\beta}$ [eV]	Collaboration
^{76}Ge	$>1.8\times10^{26}$	$<$(0.08–0.18)	GERDA [23]
^{76}Ge	$>2.7\times10^{25}$	$<$(0.2–0.433)	MAJORANA DEMONSTRATOR [116]
	$>8.3\times10^{25}$	$<$(0.113–0.269)	[117]
^{82}Se	$>3.5\times10^{24}$	$<$(0.311–0.638)	CUPID-0 [118]
^{130}Te	$>2.2\times10^{25}$	$<$(0.09–0.305)	CUORE [119]
^{136}Xe	$>3.5\times10^{25}$	$<$(0.093–0.286)	EXO [24]
^{136}Xe	$>1.07\times10^{26}$	$<$(0.061–0.165)	KamLAND-Zen [25]
	$>2.3\times10^{26}$	$<$(0.036–0.156)	[26]

In order to assess the relevance of the interference term $2\mathrm{Re}(m^{N}_{\beta\beta,R}\cdot m^{S^*}_{\beta\beta,R})$ in our study, we consider both the cases of neglecting it and of taking it into account.

We express next the three terms in the generalized effective Majorana mass in terms of the PMNS mixing angles, Dirac and Majorana *CPV* phases present in the PMNS matrix, the three light neutrino masses and, in the case of the nonstandard contributions, the masses of $N_{1,2,3}$ and of $S_{1,2,3}$.

The effective Majorana mass term for standard mechanism can be written as (see, e.g., [18,110])

$$|m^{\nu}_{\beta\beta,L}| = \left|\sum_{i=1}^{3} U^2_{ei} m_i\right| = |m_1 c^2_{12}c^2_{13} + m_2 s^2_{12}c^2_{13}e^{i\alpha} + m_3 s^2_{13}e^{i(\beta-2\delta)}|, \tag{4.16a}$$

where m_1, m_2, m_3 are masses of the light Majorana neutrinos $\nu_{1,2,3}$ and we have used the standard parametrization of the PMNS matrix. Defining

$$C_N = m_e m_p \frac{M^{0\nu}_N}{M^{0\nu}_\nu}\frac{M^4_{W_L}}{M^4_{W_R}}, \tag{4.17}$$

the expression for $m^{N}_{\beta\beta,R}$ can be cast in the form,

$$\begin{aligned}|m^{N}_{\beta\beta,R}| &= \frac{C_N}{m_{N_1}}\left|\left[U^2_{e1} + \frac{U^2_{e2}e^{i\alpha}m_{N_1}}{m_{N_2}} + \frac{U^2_{e3}e^{i\beta}m_{N_1}}{m_{N_3}}\right]\right| \\ &= \frac{C_N}{m_{N_1}}\left|\left[U^2_{e1} + \frac{U^2_{e2}e^{i\alpha}m_2}{m_1} + \frac{U^2_{e3}e^{i\beta}m_3}{m_1}\right]\right| \\ &= \frac{C_N}{m_{N_1}m_1}|m^{\nu}_{\beta\beta,L}|, \qquad \text{NO case,}\end{aligned} \tag{4.18}$$

$$\begin{aligned}|m^{N}_{\beta\beta,R}| &= \frac{C_N}{m_{N_3}}\left|\left[\frac{U^2_{e1}m_{N_3}}{m_{N_1}} + \frac{U^2_{e2}e^{i\alpha}m_{N_3}}{m_{N_2}} + U^2_{e3}e^{i\beta}\right]\right| \\ &= \frac{C_N}{m_{N_3}}\left|\left[\frac{U^2_{e1}m_1}{m_3} + \frac{U^2_{e2}e^{i\alpha}m_2}{m_3} + U^2_{e3}e^{i\beta}\right]\right| \\ &= \frac{C_N}{m_{N_3}m_3}|m^{\nu}_{\beta\beta,L}|, \qquad \text{IO case,}\end{aligned} \tag{4.19}$$

where we have used Eqs. (3.15) and (3.16). We see that in the considered setting the contribution due to exchange of the heavy Majorana neutrinos $N_{1,2,3}$ is proportional to the standard contribution due to the light Majorana neutrino exchange, $|m^{N}_{\beta\beta,R}| \propto |m^{\nu}_{\beta\beta,L}|$.

We consider next $m^{S}_{\beta\beta,R}$. It follows from Eq. (3.11) that $m_{N_i} = \frac{k^2_{rs}}{m_{S_i}}$. As it is described in the Appendix, the mixing $V^{NS}_{ek} \equiv M_{RS}M^{-1}_S U_S$. We can diagonalize M_S as $M_S = U_S M^D_S U_S{}^T$. Since $M_{RS} = k_{rs}I$, the mixing

$$\begin{aligned}V^{NS}_{ek} &= k_{rs}(U_S M^D_S U_S{}^T)^{-1}U_S \\ &= k_{rs}U^*_S \mathrm{diag}(1/m_{S_1}, 1/m_{S_2}, 1/m_{S_3}).\end{aligned} \tag{4.20}$$

Using the relation $m_{N_i} = \frac{k^2_{rs}}{m_{S_i}}$ and Eqs. (3.15)–(3.18), the expression for $m^{S}_{\beta\beta,R}$ can be written as

$$\begin{aligned}|m^{S}_{\beta\beta,R}| &= C_N k^2_{rs}\left|\left[\frac{U^2_{e1}}{m^3_{S_1}} + \frac{U^2_{e2}e^{i\alpha}}{m^3_{S_2}} + \frac{U^2_{e3}e^{i\beta}}{m^3_{S_3}}\right]\right| \\ &= \left|C_N\left[\frac{U^2_{e1}m_{N_1}}{m^2_{S_1}} + \frac{U^2_{e2}e^{i\alpha}m_{N_2}}{m^2_{S_2}} + \frac{U^2_{e3}e^{i\beta}m_{N_3}}{m^2_{S_3}}\right]\right| \\ &= \left|\frac{C_N m_{N_1}m_1m^2_3}{m^2_{S_3}m^3_1}\left[U^2_{e1} + U^2_{e2}e^{i\alpha}\frac{m^3_1}{m^3_2} + U^2_{e3}e^{i\beta}\frac{m^3_1}{m^3_3}\right]\right| \\ &\qquad \text{NO case,}\end{aligned} \tag{4.21}$$

$$\begin{aligned}|m^{S}_{\beta\beta,R}| &= \left|C_N m_{N_3}\left[\frac{U^2_{e1}}{m^2_{S_1}}\frac{m_3}{m_1} + \frac{U^2_{e2}e^{i\alpha}}{m^2_{S_2}}\frac{m_3}{m_2} + \frac{U^2_{e3}e^{i\beta}}{m^2_{S_3}}\right]\right| \\ &= \left|\frac{C_N m_{N_3}m_3m^2_2}{m^2_{S_2}m^3_3}\left[U^2_{e1}\frac{m^3_3}{m^3_1} + U^2_{e2}e^{i\alpha}\frac{m^3_3}{m^3_2} + U^2_{e3}e^{i\beta}\right]\right|, \\ &\qquad \text{IO case.}\end{aligned} \tag{4.22}$$

It follows from Eqs. (4.18)–(4.22) that $|m^{N}_{\beta\beta,R}|$ and $|m^{S}_{\beta\beta,R}|$ exhibit very unusual dependence on the lightest neutrino mass $m_{1(3)}$: $|m^{N}_{\beta\beta,R}| \propto 1/m_{1(3)}$ and $|m^{S}_{\beta\beta,R}| \propto 1/m^2_{1(3)}$. Correspondingly, the new physics contributions to the $0\nu\beta\beta$ decay amplitude are strongly enhanced at relatively small values of $m_{1(3)}$. We will discuss this dependence in greater detail in the next section. We will show, in particular, that in the considered scenario with $m_{S_k} \sim (10^2\text{–}10^4)$ GeV and $m_{N_j} \sim (1-100)$ GeV of interest, the lightest neutrino mass $m_{1(3)}$ cannot be smaller than $\sim 10^{-4}$ eV. We will also show that due to the indicated enhancement the new contributions dominate over the standard mechanism contribution for $m_{1(3)} \sim (10^{-4}\text{–}10^{-2})$ eV.[1]

V. PHENOMENOLOGICAL ANALYSIS

In the present section, we will discuss the effects of the new physics contributions to the $0\nu\beta\beta$ decay amplitude on the predictions for the effective Majorana mass and the $0\nu\beta\beta$ decay half-life. We recall that if $0\nu\beta\beta$ decay will be observed, the data on the half-life of $0\nu\beta\beta$ decay generated by the standard mechanism can provide important

[1]The effects of the heavy Majorana neutrino exchange in $0\nu\beta\beta$ decay amplitude in a left-right symmetric model setting were studied recently de Vries *et al.* [120]. However, the version of the left-right symmetric model considered by us and in de Vries *et al.* [120], differ significantly and practically there is no overlap in what concerns the results on the contributions of interest of the heavy Majorana exchange to the $0\nu\beta\beta$ decay amplitude.

information on the absolute scale of light neutrino masses and on the neutrino mass ordering [121,122]. With additional input data about the values of the lightest neutrino mass $m_{1(3)}$ (or the sum of the neutrino masses), it might be possible to get information about the values of the Majorana phases in the PMNS matrix as well [18,123]. In what follows, we will investigate, in particular, how the quoted results are possibly modified by the new contributions to the $0\nu\beta\beta$ decay amplitude.

A. Mass parameter ranges

We note first that there exist rather stringent constrains on coupling and masses of the heavy Majorana neutrinos associated with the low-scale type-I seesaw mechanism of neutrino mass generation which have been comprehensively discussed in [124]. In the model studied by us the heavy Majorana neutrinos have masses greater than 1 GeV. The couplings of the heavy Majorana neutrino states in the left-handed $(V-A)$ charged lepton current are suppressed, being smaller than $\sim 10^{-6}$. Their couplings in the right-handed $(V+A)$ charged current are not suppressed being $\sim U_{\rm PMNS}$, but the contribution of the $(V+A)$ charged current interaction to the rates of experimentally measured observables is suppressed by the factor $(M_{W_L}/M_{W_R})^4 < 10^{-8}$, where $M_{W_L} = 80.38$ GeV in the mass of the Standard Model $W^{\pm}$ boson, while M_{W_R} is the mass of its $SU(2)_R$ counterpart, and we have used the constraint $M_{W_R} > 5$ TeV following from the LHC data. As a consequence, the low-energy experimental constrains on the heavy Majorana neutrinos summarized in [124] are satisfied in the model considered by us and do not lead to additional restrictions on the couplings and/or masses of these states.

The new nonstandard contributions to the $0\nu\beta\beta$ decay amplitude, $|m^N_{\beta\beta,R}|$ and $|m^S_{\beta\beta,R}|$, as it follows from Eqs. (4.18)–(4.22), have very peculiar dependence on the lightest neutrino mass $m_{1(3)}$. They are strongly enhanced and, as we are going to show below, are considerably larger that the standard mechanism contribution $|m^{\nu}_{\beta\beta,L}|$ at $m_{1(3)} \lesssim 10^{-3}$ eV, where $|m^N_{\beta\beta,R}| > |m^{\nu}_{\beta\beta,L}|$, $|m^S_{\beta\beta,R}| \gg |m^{\nu}_{\beta\beta,L}|$, and $|m^S_{\beta\beta,R}| \gg |m^N_{\beta\beta,R}|$. At $m_{1(3)} \gtrsim 5\times 10^{-2}$ eV, however, we have $|m^N_{\beta\beta,R}|, |m^S_{\beta\beta,R}| \ll |m^{\nu}_{\beta\beta,L}|$. This implies that the most stringent conservative experimental upper limit on $|m^{0\nu}_{\beta\beta}| < 0.156$ eV reported by the KamLAND-Zen collaboration [26] (see Table IV) applies to $|m^{\nu}_{\beta\beta,L}|$ since it corresponds to light neutrino masses $m_{1,2,3} \gtrsim 0.1$ eV. Actually, it follows from the quoted upper limit that [88,125] $m_{1,2,3} \lesssim 0.156/(\cos 2\theta_{12} - \sin^2\theta_{13}) \cong 0.55$ eV, where we have used the 3σ allowed ranges of $\sin^2\theta_{12}$ and $\sin^2\theta_{13}$ given in Table II neglecting the minor differences in the ranges corresponding to NO and IO neutrino mass spectra. Thus, the largest light neutrino mass $m_{3(2)}$ is allowed to vary approximately between $\sqrt{\Delta m^2_{31(23)}} \cong 5\times 10^{-2}$ eV and 0.55 eV.

The CMB data of WMAP and PLANCK experiments, combined with supernovae and other cosmological and astrophysical data can be used to obtain information in the form of an upper limit on the sum of neutrinos masses and thus on $m_{3(2)}$ (see e.g., Ref. [126]). Depending on the model complexity and the input data used one typically finds [127] (see also [128]) $\sum_j m_j < (0.12\text{–}0.54)$ eV (95% C.L.). The quoted conservative upper limit on $\sum_j m_j$ implies $m_{3(2)} \lesssim 0.18$ eV. In our phenomenological and numerical analysis, we will use somewhat larger values of $m_{3(2)}$, keeping in mind the existence of more stringent limits. We recall further that in the model considered by us $m_{N_i} = k_d^2/m_i$, $m_{S_i} = (k_{rs}^2/k_d^2)m_i$, where k_d and k_{rs} are real constant parameters. Correspondingly, in the case of NO light neutrino mass spectrum, $m_1 < m_2 < m_3$, we have $m_{N_3} < m_{N_2} < m_{N_1}$ and $m_{S_1} < m_{S_2} < m_{S_3}$. For IO spectrum, $m_3 < m_1 < m_2$, we have instead $m_{N_2} < m_{N_1} < m_{N_3}$ and $m_{S_3} < m_{S_1} < m_{S_2}$. In the double seesaw model under discussion, we should always have in the NO (IO) case $m_{N_{1(2)}} \ll m_{S_{3(2)}}$, i.e., $m_{S_{3(2)}} \gtrsim 10 m_{N_{1(2)}}$.

In what follows, we will consider the values of $m_{S_{3(2)}}$ and $m_{N_{1(3)}}$ in the intervals (1–10) TeV and $(10^2\text{–}10^3)$ GeV, respectively, while the mass of the lightest RH Majorana neutrino $N_{3(2)}$ will be assumed to satisfy $m_{N_{3(2)}} \geq 1$ GeV. The minimal value of $m_{N_{3(2)}}$ of 1 GeV should correspond to the maximally allowed value of $m_{3(2)} \cong 0.55$ eV considered by us. As a consequence, we have $k_d^2 = \min(m_{N_{3(2)}})\max(m_{3(2)}) = 0.55$ eV GeV. We get similar value of k_d^2 if we use $m_{N_{3(2)}} = 10$ GeV and $m_{3(2)} \cong 0.05$ eV. Given the value of k_d^2, the requirement that the mass of the heaviest RH Majorana neutrino $m_{N_{1(3)}}$ should not exceed 10^3 GeV implies a lower limit on the mass of the lightest Majorana neutrino $m_{1(3)}$: $m_{1(3)} = k_d^2/m_{N_{1(3)}} \gtrsim 0.55\times 10^{-3}$ eV. Thus, for consistency with the chosen ranges of value of the heavy Majorana fermions in the model, the value of the lightest neutrino mass should not be smaller than about 5.5×10^{-4} eV. In the numerical analysis, we will perform we will exploit the range $m_{1(3)} = (10^{-4}\text{–}1.0)$ eV.

In the analysis which follows, we will use the values of the neutrino oscillation parameters given in Table II. We set the Dirac phase $\delta = 0$. The Majorana phases α and β are varied in the interval $[0,\pi]$. For the parameters M_{W_R}, $m_{N_{1(3)}}$, $m_{S_{3(2)}}$ and the ratio $M^{0\nu}_N/M^{0\nu}_{\nu}$ the following reference values will be utilized: $M_{W_R} = 5.5$ TeV, $m_{N_{1(3)}} = 300$ GeV, $m_{S_{3(2)}} = 3$ TeV, and $M^{0\nu}_N/M^{0\nu}_{\nu} \cong 22.2\text{–}76.3$ (concerning $M^{0\nu}_N/M^{0\nu}_{\nu}$, see Eq. (4.7) and the discussion related to it).

B. Light neutrino contribution

The phenomenology of the light neutrino contribution to the $0\nu\beta\beta$ decay half-life, including the properties of the corresponding effective Majorana mass $|m^{\nu}_{\beta\beta,L}|$ have been extensively studied and are well-known (see e.g., [88]). In this subsection, we summarize the main features of $|m^{\nu}_{\beta\beta,L}|$.

C. Normal ordering

In this case $|m^{\nu}_{\beta\beta,L}|$ (see Eq. (4.16) can be rewritten in terms of neutrino mass square differences as

$$|m^{\nu}_{\beta\beta,L}| = |m_1 c^2_{12} c^2_{13} + \sqrt{m_1^2 + \Delta m^2_{21}} s^2_{12} c^2_{13} e^{i\alpha} + \sqrt{m_1^2 + \Delta m^2_{31}} s^2_{13} e^{i\beta}|. \quad (5.1)$$

The best-fit values and the 3σ allowed ranges of $s^2_{12} \equiv \sin^2\theta_{12}$, $s^2_{13} \equiv \sin^2\theta_{13}$, and of Δm^2_{21} and Δm^2_{31} are given in Table II.

The case of hierarchical light neutrino mass spectrum corresponds to $m_1 \ll m_2 < m_3$. In this case $m_2 \approx \sqrt{\Delta m^2_{21}} \approx 8.57 \times 10^{-3}$ eV and $m_3 \approx \sqrt{\Delta m^2_{31}} \approx 4.98 \times 10^{-2}$ eV, and thus $m_1 \lesssim 8 \times 10^{-4}$ eV. Depending on the values of the Majorana phases, $|m^{\nu}_{\beta\beta,L}|$ can take values in the interval $(0.4\text{–}4.8) \times 10^{-3}$ eV, where we have used the 3σ allowed ranges of the relevant oscillation parameters. At $m_1 = 10^{-4}$ eV we have 0.91×10^{-3} eV $\lesssim |m^{\nu}_{\beta\beta,L}| \lesssim 4.37 \times 10^{-3}$ eV.

The effective Majorana mass $|m^{\nu}_{\beta\beta,L}|$ exhibits strong dependence on the values of the Majorana phases α and β in the case of NO neutrino mass spectrum with partial hierarchy corresponding to $m_1 = (10^{-3}\text{–}10^{-2})$ eV. Indeed, for $\alpha = \pi$ and $\beta = 0$, $|m^{\nu}_{\beta\beta,L}|$ is strongly suppressed for values of m_1 lying in the interval $(1.3\text{–}9.0) \times 10^{-3}$ eV, where $|m^{\nu}_{\beta\beta,L}| \lesssim 2 \times 10^{-4}$ eV due to cancellations (partial or complete) between the three terms in the expression of $|m^{\nu}_{\beta\beta,L}|$. Using the best-fit values of the neutrino oscillation parameters, we find that a complete cancellation takes place and $|m^{\nu}_{\beta\beta,L}| = 0$ at $m_1 \cong 2.26 \times 10^{-3}$ eV. At the same time, at $m_1 = 2.26(9.0) \times 10^{-3}$ eV, for example, $|m^{\nu}_{\beta\beta,L}| \approx 5(10) \times 10^{-3}$ eV if $\alpha = 0$ and $\beta = 0$.

As m_1 increases beyond 10^{-2} eV, $|m^{\nu}_{\beta\beta,L}|$ increases almost linearly with m_1 and at $m_1 \cong 0.1$ eV enters the quasidegenerate neutrino mass spectrum region where $|m^{\nu}_{\beta\beta,L}| \gtrsim 0.05$ eV.

D. Inverted ordering

In this case we have

$$|m^{\nu}_{\beta\beta,L}| = \Big| \sqrt{m_3^2 + \Delta m^2_{23} - \Delta m^2_{21}} c^2_{12} c^2_{13} + \sqrt{m_3^2 + \Delta m^2_{23}} s^2_{12} c^2_{13} e^{i\alpha} + m_3 s^2_{13} e^{i\beta}) \Big|. \quad (5.2)$$

The behavior of $|m^{\nu}_{\beta\beta,L}|$ as a function of the lightest neutrino mass m_3 is very different from the behavior in the NO case. Given the fact that $m_2 = \sqrt{m_3^2 + \Delta m^2_{23}} \gtrsim 5 \times 10^{-2}$ eV, $m_1 = \sqrt{m_3^2 + \Delta m^2_{23} - \Delta m^2_{21}} \gtrsim 5 \times 10^{-2}$ eV, $s^2_{13} \cong 0.022$ and at 3σ we have $(c^2_{12} - s^2_{12}) \gtrsim 0.31$, complete cancellation between the three terms in Eq. (5.2) is not possible. Actually, at $m_3^2 \ll \Delta m^2_{23}$, or equivalently, at $m_3 \lesssim 1.6 \times 10^{-2}$ eV, $|m^{\nu}_{\beta\beta,L}|$ practically does not depend on m_3. At these values of m_3 we have $\sqrt{\Delta m^2_{23}} \cos 2\theta_{12} \lesssim |m^{\nu}_{\beta\beta,L}| \lesssim \sqrt{\Delta m^2_{23}}$. Using the 3σ allowed ranges of $\sqrt{\Delta m^2_{23}}$ and $\cos 2\theta_{12}$ from Table II we get: 1.51×10^{-2} eV $\lesssim |m^{\nu}_{\beta\beta,L}| \lesssim 5.06 \times 10^{-2}$ eV.

If the $0\nu\beta\beta$ decay were generated by the standard mechanism only, the fact that in the case of hierarchical light neutrino mass spectrum the minimal value of $|m^{\nu}_{\beta\beta,L}|$ for the IH spectrum is approximately by a factor of 3.4 larger than the maximal value of $|m^{\nu}_{\beta\beta,L}|$ for the NH spectrum opens up the possibility of obtaining information about the type of neutrino mass spectrum from a measurement of $|m^{\nu}_{\beta\beta,L}|$ [121].

As m_3 increases beyond 1.6×10^{-2} eV, $|m^{\nu}_{\beta\beta,L}|$ also increases and at $m_3 \cong 0.1$ eV enters the QD region where $|m^{\nu}_{\beta\beta,L}| \gtrsim 0.03$ eV growing linearly with m_3.

E. The contribution due to the exchange of $N_{1,2,3}$

The contribution due to the exchange of virtual $N_{1,2,3}$ in the NO and IO cases are given respectively in Eqs. (4.18) and (4.19) can be cast in the form,

$$|m^{N}_{\beta\beta,R}| = \frac{C_N}{m_{N_{1(3)}} m_{1(3)}} |m^{\nu}_{\beta\beta,L}|, \qquad \text{NO (IO) case}, \quad (5.3)$$

where C_N is defined in Eq. (4.17) and $|m^{\nu}_{\beta\beta,L}|$ is the effective Majorana mass associated with the standard mechanism discussed in the preceding subsection. Using the $M_{W_L} = 80.38$ GeV, the reference values of $M_{W_R} = 5.5$ TeV we get

$$\frac{C_N}{m_{N_{1(3)}} m_{1(3)}} \cong 0.729 \left(\frac{m_{N_{1(3)}}}{300\ \text{GeV}}\right)^{-1} \left(\frac{m_{1(3)}}{10^{-4}\ \text{eV}}\right)^{-1} \frac{M^{0\nu}_N}{M^{0\nu}_\nu}. \quad (5.4)$$

Taking into account the minimal and maximal reference values of $M^{0\nu}_N / M^{0\nu}$ in Eq. (4.7) and fixing $m_{N_{1(3)}}$ to the reference value of 300 GeV, the variation of the factor $C_N/(m_{N_{1(3)}} m_{1(3)})$ with the change of lightest neutrino mass is displayed in Fig. 2. We also estimate the possible range of values of the factor $C_N/(m_{N_{1(3)}} m_{1(3)})$ for four values of the lightest neutrino mass $m_{1(3)}$ as follows:

$C_N/(m_{N_{1(3)}} m_{1(3)}) \cong (16.2 - 55.6)$ for $m_{1(3)} = 10^{-4}$ eV,
$C_N/(m_{N_{1(3)}} m_{1(3)}) \cong (1.62 - 5.56)$ for $m_{1(3)} = 10^{-3}$ eV,

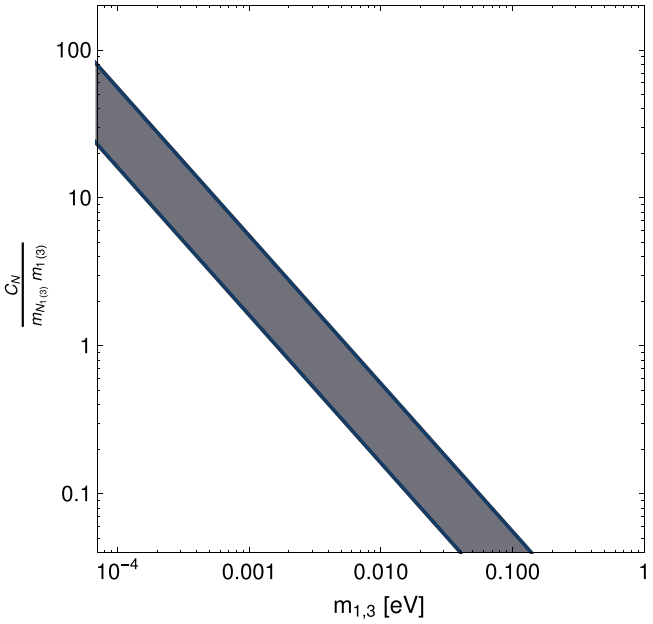

FIG. 2. The plot for $C_N/(m_{N_{1(3)}} m_{1(3)}$ with the change of lightest neutrino mass $(m_{1(3)})$ for the reference value of $m_{N_{1(3)}} = 300$ GeV and that band corresponds to varying $M_N^{0\nu}/M_\nu^{0\nu}$ in the interval $22.2 \leq M_N^{0\nu}/M_\nu^{0\nu} \leq 76.3$ as given in Eq. (4.7).

$C_N/(m_{N_{1(3)}} m_{1(3)}) \cong (0.32 - 1.11)$ for $m_{1(3)} = 5\times 10^{-3}$ eV, and
$C_N/(m_{N_{1(3)}} m_{1(3)}) \cong (0.16 - 0.56)$ for $m_{1(3)} = 10^{-2}$ eV.

It is clear from these estimates that for 10^{-4} eV $\leq m_{1(3)} \leq 10^{-3}$ eV, the contribution due to exchange of virtual $N_{1,2,3}$ is larger than the standard mechanism contribution, $|m^N_{\beta\beta,R}| > |m^\nu_{\beta\beta,L}|$. For $m_{1(3)} \sim (10^{-4} - 5\times 10^{-4})$ eV we have actually $|m^N_{\beta\beta,R}| \gg |m^\nu_{\beta\beta,L}|$. In this interval of values of m_1 in the NO case, $|m^N_{\beta\beta,R}|$ lies in the region corresponding to the IO neutrino mass spectrum if only the standard mechanism (i.e., only light Majorana neutrino exchange) were operative in $0\nu\beta\beta$ decay. The predicted values of $|m^N_{\beta\beta,R}|$ in the IO case are larger than the experimental limits on effective Majorana mass reported by the GERDA and KamLAND-Zen experiments (see Table IV).

In the region $m_{1(3)} \sim (10^{-3}$–$10^{-2})$ eV we have roughly $|m^N_{\beta\beta,R}| \sim |m^\nu_{\beta\beta,L}|$ (see below), with $|m^N_{\beta\beta,R}|$ decreasing as $1/m_{1(3)}$. In the NO case, $|m^\nu_{\beta\beta,L}|$ can be strongly suppressed, i.e., depending on the values of the Majorana phases it can have value $|m^\nu_{\beta\beta,L}| \leq 10^{-4}$ eV, and in this case $|m^N_{\beta\beta,R}|$ will also be suppressed. At $m_1 = 10^{-3}$ eV though at which $|m^\nu_{\beta\beta,L}| \cong 3\times 10^{-4}$ eV, $|m^N_{\beta\beta,R}|$ can be somewhat larger than $|m^\nu_{\beta\beta,L}|$ owing to the relevant NME element ratio and can have a value $|m^N_{\beta\beta,R}| \cong 1.5\times 10^{-3}$ eV. In the IO case, $|m^N_{\beta\beta,R}| \gtrsim |m^\nu_{\beta\beta,L}|$ in the discussed region. It can be larger than $|m^\nu_{\beta\beta,L}|$ by a factor of 2.

At $m_{1(3)} > 10^{-2}$ eV, $|m^\nu_{\beta\beta,L}| \gtrsim |m^N_{\beta\beta,R}|$ and at $m_{1(3)} \geq 5\times 10^{-2}$ eV, we have $|m^\nu_{\beta\beta,L}| \gg |m^N_{\beta\beta,R}|$ and the contribution due to the exchange of $N_{1.2.3}$ is subleading and practically negligible in both NO and IO cases.

For values of $m_{N_{1(3)}}$ smaller (larger) than the considered 300 GeV, $|m^N_{\beta\beta,R}|$ will have values which are larger (smaller) than those discussed above by the factor 300 GeV$/m_{N_{1(3)}}$. Since in the considered scenario the mass of the lightest N_j is assumed to satisfy $m_{N_{3(2)}} \geq 1$ GeV and is given by $m_{N_{3(2)}} = (m_{1(3)}/m_{3(2)})m_{N_{1(3)}}$, $m_{1(3)} \gtrsim 5.5\times 10^{-4}$ eV, and from the data it follows that $m_{3(2)} \gtrsim 5\times 10^{-2}$ eV, for consistency one should have also $m_{N_{1(3)}} \gtrsim 100$ GeV.

F. The contribution due to the exchange of $S_{1.2.3}$

The important parameter for the contribution due to the exchange of $S_{1.2.3}$ in the NO (IO) case is the dimensionful factor

$$C_S^{\mathrm{NO(IO)}} \equiv \frac{C_N m_{N_{1(3)}} m_{1(3)} m^2_{3(2)}}{m^2_{S_{3(2)}} m^3_{1(3)}}, \qquad \mathrm{NO\,(IO)}. \tag{5.5}$$

Taking into account Eq. (5.4), $C_S^{\mathrm{NO(IO)}}$ can be cast in the form,

$$C_S^{\mathrm{NO(IO)}} = 0.729\times 10^{-6}\ \mathrm{eV}\frac{m_{N_{1(3)}}}{300\ \mathrm{GeV}}\left(\frac{m_{S_{3(2)}}}{3\ \mathrm{TeV}}\right)^{-2} \times\left(1+\frac{\Delta m^2_{31(23)}}{m^2_{1(3)}}\right)\frac{M_N^{0\nu}}{M_\nu^{0\nu}}, \qquad \mathrm{NO\,(IO)}. \tag{5.6}$$

Setting $m_{N_{1(3)}}$, $m_{S_{3(2)}}$, M_{W_R} to the reference values of 300 GeV, 3 TeV, and 5.5 TeV, respectively and using the values of $\Delta m^2_{31(23)} \cong 2.5\times 10^{-3}\mathrm{eV}^2$ (see Table II) and $\mathrm{M_N^{0\nu}/M^{0\nu}}$ as given in Eq. (4.7), the variation of $C_S^{\mathrm{NO(IO)}}$ with the change of lightest neutrino mass is shown in Fig. 3. Using these reference model parameters we calculate the factor $C_S^{\mathrm{NO(IO)}}$ for different values of lightest neutrino mass as given below, $C_S^{\mathrm{NO(IO)}} \cong (4.05 - 13.90)$ eV for $m_{1(3)} = 10^{-4}$ eV, $C_S^{\mathrm{NO(IO)}} \cong (0.040$–$0.139)$ eV for $m_{1(3)} = 10^{-3}$ eV, $C_S^{\mathrm{NO(IO)}} \cong (4.21\times 10^{-4}$–$1.45\times 10^{-3})$eV for $m_{1(3)} = 10^{-2}$ eV, $C_S^{\mathrm{NO(IO)}} \cong (3.24\times 10^{-5} - 1.11\times 10^{-4})$ eV for $m_{1(3)} = 5\times 10^{-2}$ eV, $C_S^{\mathrm{NO(IO)}} \cong (2.0 - 6.9)\times 10^{-5})$ eV for $m_{1(3)} = 10^{-1}$ eV.

It follows from these numerical estimates that $C_S^{\mathrm{NO(IO)}}$, and thus $|m^S_{\beta\beta,R}|$, decreases rapidly with the increase of $m_{1(3)}$ in the interval $(10^{-4} - 5\times 10^{-2})$ eV.

We recall that the contributions due to the exchange of $S_{1.2.3}$ in the NO and IO cases are given by

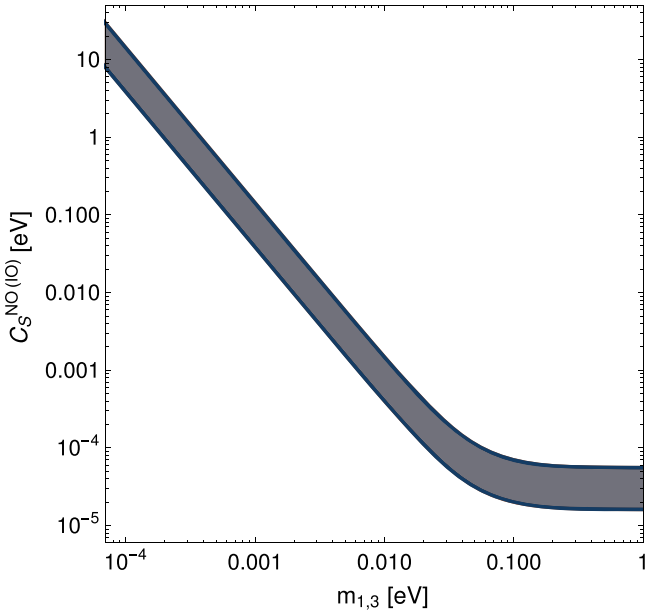

FIG. 3. Variation of C_S with the lightest neutrino mass (m_1 for NO and m_3 for IO) obtained by setting $m_{N_{1(3)}}$, $m_{S_{3(2)}}$, and M_{W_R} to the reference values of 300 GeV, 3 TeV, and 5.5 TeV, respectively and $\Delta m^2_{31(23)} \cong 2.5 \times 10^{-3}\text{eV}^2$ (see Table II). The solid band is obtained by varying the ratio $M_N^{0\nu}/M_\nu^{0\nu}$ in the range, $22.2 \leq \mathrm{M}_\mathrm{N}^{0\nu}/\mathrm{M}_\nu^{0\nu} \leq 76.3$ as given in Eq. (4.7).

$$|m^S_{\beta\beta,R}| = C_\mathrm{S}^\mathrm{NO}\left|U^2_{e1} + U^2_{e2}e^{i\alpha}\frac{m_1^3}{m_2^3} + U^2_{e3}e^{i\beta}\frac{m_1^3}{m_3^3}\right| \quad \text{NO case,} \tag{5.7}$$

$$|m^S_{\beta\beta,R}| = C_\mathrm{S}^\mathrm{IO}\left|U^2_{e1}\frac{m_3^3}{m_1^3} + U^2_{e2}e^{i\alpha}\frac{m_3^3}{m_2^3} + U^2_{e3}e^{i\beta}\right| \quad \text{IO case,} \tag{5.8}$$

and that $|U_{e1}|^2 \cong 0.7$ and $|U_{e3}|^2 \cong 0.022$.

Consider the NO case. We note first that with the increasing of m_1 beyond 10^{-2} eV, the contribution $|m^S_{\beta\beta,R}|$ to the $0\nu\beta\beta$ decay amplitude becomes subdominant and negligible. For $m_1 = (10^{-4}$–$10^{-2})$ eV, the ratio $m_1^3/m_3^3 \ll 1$, while $m_1^3/m_2^3 \ll 1$ in the interval $m_1 = (10^{-4} - 4.5 \times 10^{-3})$ eV. This implies that for $m_1 \lesssim 4.5 \times 10^{-3}$ eV, the second and third terms in the expression (5.7) for $|m^S_{\beta\beta,R}|$ are practically negligible and $|m^S_{\beta\beta,R}| \cong C_\mathrm{S}^\mathrm{NO}|U_{e1}|^2$ with essentially no dependence on the Majorana phases. In the interval $m_1 = (4.5 \times 10^{-3}$–$10^{-2})$ eV the ratio m_1^3/m_2^3 increases with m_1 and at $m_1 = 10^{-2}$ eV we have $m_1^3/m_2^3 \cong 0.44$. Thus, even at this value the maximal effect of the Majorana phases is to change the value of $|U_{e1}|^2 \cong 0.7$ to $|U_{e1}|^2 \pm m_1^3/m_2^3|U_{e2}|^2$, or to 0.70 ± 0.13, i.e., by at most 18%, where we have used the best-fit values of $\sin^2\theta_{12}$ and $\sin^2\theta_{13}$. Thus, in the interval of values of m_1 of interest, where the contribution of $|m^S_{\beta\beta,R}|$ is important, there can not be significant compensation between the three terms in the expression for $|m^S_{\beta\beta,R}|$.

From the numerical estimates of $|m^\nu_{\beta\beta,L}|$, $|m^N_{\beta\beta,R}|$ and $|m^S_{\beta\beta,R}|$ in the preceding and current subsections, it follows that in the interval of interest $m_1 = (10^{-4}$–$10^{-2})$ eV, we have $|m^S_{\beta\beta,R}| > (\gg)|m^\nu_{\beta\beta,L}|, |m^N_{\beta\beta,R}|$. This is particularly important in the interval 10^{-3} eV $< m_1 < 10^{-2})$ eV, where $|m^\nu_{\beta\beta,L}| < 3 \times 10^{-4}$ eV, while $|m^S_{\beta\beta,R}| \gtrsim 3 \times 10^{-4}$ eV and, depending on the NME, at $m_1 = 10^{-3}$ eV can be as large as $|m^S_{\beta\beta,R}| \cong 9.7 \times 10^{-2}$ eV $\gg |m^\nu_{\beta\beta,L}|, |m^N_{\beta\beta,R}|$.

The situation is very different in the IO case. In the interval $m_3 = (10^{-4}$–$10^{-2})$ eV, where the factor C_S^IO has a relatively large value, we have $(m_3/m_{2(1)})^3 \lesssim 7.5 \times 10^{-3}$, which implies that actually $|m^S_{\beta\beta,R}| \cong C_\mathrm{S}^\mathrm{IO}|U_{e3}|^2 \cong 2.2 \times 10^{-2} C_\mathrm{S}^\mathrm{IO}$. As a consequence of the suppression due to $|U_{e3}|^2$ we have in the interval of values of m_3 of interest $|m^S_{\beta\beta,R}| \ll |m^N_{\beta\beta,R}|$.

G. The contribution of the interference term

The contribution of the interference term $2\mathrm{Re}(m^N_{\beta\beta,R} \cdot m^{S^*}_{\beta\beta,R})$ in Eq. (4.15) in the $0\nu\beta\beta$ decay rate may be non-negligible only in the interval of values of $m_{1(3)} = (10^{-4}$–$10^{-2})$ eV, where the new nonstandard contributions are significant. Using the analytical expressions for $|m^N_{\beta\beta,R}|$ and $|m^S_{\beta\beta,R}|$ in Eqs. (4.18)–(4.22) and the results reported in the preceding subsections, it is not difficult to estimate the relative magnitude of the contribution of this term. Our results show that it varies significantly with the type of neutrino mass spectrum, the values of the lightest neutrino mass $m_{1(3)}$ and of the Majorana phases α and β.

The relative contribution of the interference term of interest is determined by the ratio

$$R \equiv \frac{2\mathrm{Re}(m^N_{\beta\beta,R} \cdot m^{S^*}_{\beta\beta,R})}{|m^\nu_{\beta\beta,L}|^2 + |m^N_{\beta\beta,R}|^2 + |m^S_{\beta\beta,R}|^2}. \tag{5.9}$$

Using the ratio R, the generalized effective Majorana mass defined in Eq. (4.15) can be written as

$$m_{ee}^{\nu+|N+S|} = m_{ee}^{\nu+N+S}\sqrt{1+R}. \tag{5.10}$$

In the case of NO spectrum, the sign of the interference term of interest depends on the Majorana phases α and β. For $\alpha = \beta = 0$, the ratio $R < 0$ and thus, the interference terms give a negative contribution to the $0\nu\beta\beta$ decay rate. The magnitude of this contribution increases quickly when m_1 increases from 10^{-4} eV to 10^{-3} eV with R changing from (-0.044) to (-0.48). The effect of the interference term peaks at $m_1 \cong 2 \times 10^{-3}$ eV where $R \cong -0.85$. Thus,

at this value of m_1 we have the maximal suppression of $m_{ee}^{\nu+N+S}$ by the factor $\sqrt{1+R}$: $m_{ee}^{\nu+|N+S|} \cong 0.39 m_{ee}^{\nu+N+S}$. The ratio R decreases rapidly when m_1 increases beyond 5×10^{-3} eV at which $R \cong -0.48$. The quoted values of R at $m_1 = 10^{-4}$ eV and $m_1 = 10^{-3}$ eV are essentially independent of the value of the ratio $M_N^{0\nu}/M_\nu^{0\nu}$ lying in the reference interval (22.2–76.3). The value of R quoted at $m_1 = 5\times10^{-3}$ eV corresponds to $M_N^{0\nu}/M_\nu^{0\nu} = 76.3$; for $M_N^{0\nu}/M_\nu^{0\nu} = 22.2$ it is significantly smaller in magnitude: $R \cong -0.089$.

The effect of the interference term is quite different for $\alpha = \pi$, $\beta = 0$. In this case, the interference terms give a positive contribution to the $0\nu\beta\beta$ decay rate for $m_1 < 2.26\times10^{-3}$ eV where $R > 0$. At $m_1 \cong 2.26\times10^{-3}$ eV it goes through zero ($R = 0$) since at this value $m_{\beta\beta,L}^{\nu} \cong 0$ and thus $m_{\beta\beta,R}^{N} \cong 0$. Correspondingly, at $m_1 \cong 2.26\times10^{-3}$ eV the generalized effective Majorana mass [Eq. (4.15)] $m_{ee}^{\nu+|N+S|} \cong m_{\beta\beta,R}^{S} \cong C_{\rm S}^{\rm NO} U_{e1}^2$. Taking into account that $U_{e1}^2 \cong \cos^2\theta_{12} \cong 0.7$ and using Eq. (5.6), for the reference values of $m_{N_1} = 300$ GeV, $m_{S_3} = 3$ TeV, $M_{W_R} = 5.5$ TeV, and $M_N^{0\nu}/M_\nu^{0\nu} = 22.2(76.3)$ we find $m_{ee}^{\nu+|N+S|} \cong 5.3(18.8)\times10^{-3}$ eV. At $m_1 > 2.26\times10^{-3}$ eV the interference term is negative ($R < 0$). It increases in magnitude as m_1 increases in the interval $m_1 = 3.5\times10^{-3}$–10^{-2} eV and, e.g., at $m_1 = 10^{-2}$ eV we have $R \cong -0.02(-0.16)$ for $M_N^{0\nu}/M_\nu^{0\nu} = 22.2(76.3)$. At $m_1 > 10^{-2}$ eV we have $|R| \ll 1$ and the interference term has a subleading (practically negligible) contribution in the $0\nu\beta\beta$ decay rate.

The results for the ratio R of interest are very different in the IO case. It is maximal in magnitude at $m_3 = 10^{-4}$ eV, where $R \cong -0.54$. However, for $m_3 \sim 10^{-4}$ eV, the predicted values of the generalized effective Majorana mass $|m_{ee}^{\nu+|N+S|}|$ [see Eq. (4.15)], as we will show in the next section, are strongly disfavored (practically ruled out) by the existing upper limits from the KamLAND-Zen and GERDA experiments (see Table IV and Fig. 2). In the region of values of $m_3 \gtrsim 10^{-3}$ eV, where the predictions for the generalized effective Majorana mass are compatible with the current experimental upper limits one has $|R| < 0.06$, with the value of $|R|$ decreasing rapidly with the increasing of m_3. Thus, in the IO case, the interference term under discussion has at most, a subleading (practically negligible) effect on the $0\nu\beta\beta$ half-life in the interval of values of m_3 where the predictions of the model considered are compatible with the existing lower limits on the half-life.

H. Numerical results

It follows from the analyses performed in the preceding four subsections in particular, that in the NO case the contribution due to the $S_{1,2,3}$ exchange, $|m_{\beta\beta,R}^{S}|$, dominates over the light neutrino ν_i and $N_{1,2,3}$ exchange contributions for 10^{-4} eV $\leq m_1 \lesssim 1.5\times10^{-3}$ eV. As a consequence, in the indicated interval of values of m_1 the generalized effective Majorana mass $|m_{ee}^{\nu+|N+S|}|$ exhibits weak dependence on the Majorana phases α and β since $|m_{\beta\beta,R}^{S}|$ practically does not depend on these phases. At $m_1 \gtrsim 2\times10^{-3}$ eV, for $\alpha = \beta = 0$, the $S_{1,2,3}$ contribution is subleading and

$$m_{ee}^{\nu+|N+S|} \cong \sqrt{|m_{\beta\beta,L}^{\nu}|^2 + |m_{\beta\beta,R}^{N}|^2} \cong |m_{\beta\beta,L}^{\nu}|\left(1+\frac{C_N}{m_{N_1} m_1}\right)^{\frac{1}{2}}, \quad \text{NO}, \quad \alpha=\beta=0, \tag{5.11}$$

where we have used Eq. (5.3). For $\alpha = \pi$, $\beta = 0$, however, $|m_{\beta\beta,L}^{\nu}|$ is strongly suppressed in the interval $m_1 \cong (1.5\times10^{-3} - 9\times10^{-3})$ eV and goes through zero at $m_1 \cong 2.26\times10^{-3}$ eV, where the value of m_1 is obtained using the best-fit values of the neutrino oscillations parameters. Therefore $|m_{\beta\beta,R}^{S}|$ gives significant contribution to $m_{ee}^{\nu+|N+S|}$ in the indicated interval and determines the minimal value of $m_{ee}^{\nu+|N+S|}$. At $m_1 \cong 2.26\times10^{-3}$ eV, e.g., we have $|m_{ee}^{\nu+|N+S|}| \cong |m_{\beta\beta,R}^{S}| \cong C_{\rm S}^{\rm NO}|U_{e1}|^2$.

In contrast, in the IO case the contribution due to the $S_{1,2,3}$ exchange $|m_{\beta\beta,R}^{S}|$ and of the interference term $2{\rm Re}(m_{\beta\beta,R}^{N}\cdot m_{\beta\beta,R}^{S^*})$ in the interval of values of m_3 of interest are practically negligible. Thus, for the generalized effective Majorana mass is given by

$$m_{ee}^{\nu+|N+S|} \cong \sqrt{|m_{\beta\beta,L}^{\nu}|^2 + |m_{\beta\beta,R}^{N}|^2} \cong |m_{\beta\beta,L}^{\nu}|\left(1+\frac{C_N}{m_{N_3} m_3}\right)^{\frac{1}{2}}, \quad \text{IO}. \tag{5.12}$$

In this case $|m_{ee}^{\nu+|N+S|}|$ depends significantly on the Majorana phases.

The conclusions regarding the new nonstandard contributions due to the exchange of virtual heavy Majorana fermions $N_{1,2,3}$ and $S_{1,2,3}$ to the $0\nu\beta\beta$ decay generalized effective Majorana mass and half-life reached in the phenomenological analysis are confirmed by our numerical results. These are illustrated in Fig. 4. In the three upper panels of Fig. 4 we show (i) $m_{ee}^{\nu} \equiv |m_{\beta\beta,L}^{\nu}|$ (left panel), (ii) $m_{ee}^{\nu+N+S} \equiv \sqrt{|m_{\beta\beta,L}^{\nu}|^2 + |m_{\beta\beta,R}^{N}|^2 + |m_{\beta\beta,R}^{S}|^2}$ (middle panel), and (iii) $m_{ee}^{\nu+|N+S|} \equiv \sqrt{|m_{\beta\beta,L}^{\nu}|^2 + |m_{\beta\beta,R}^{N} + m_{\beta\beta,R}^{S}|^2}$ (right panel), as functions of the lightest neutrino mass $m_{1(3)}$ in the case of NO (IO) light neutrino mass spectrum. Thus, the upper-left panel shows the dependence on $m_{1(3)}$ of the standard mechanism effective Majorana mass, while in the upper middle and right panels, the dependence of the generalized effective Majorana mass (GEMM) in which the contributions due to the exchange of the heavy Majorana

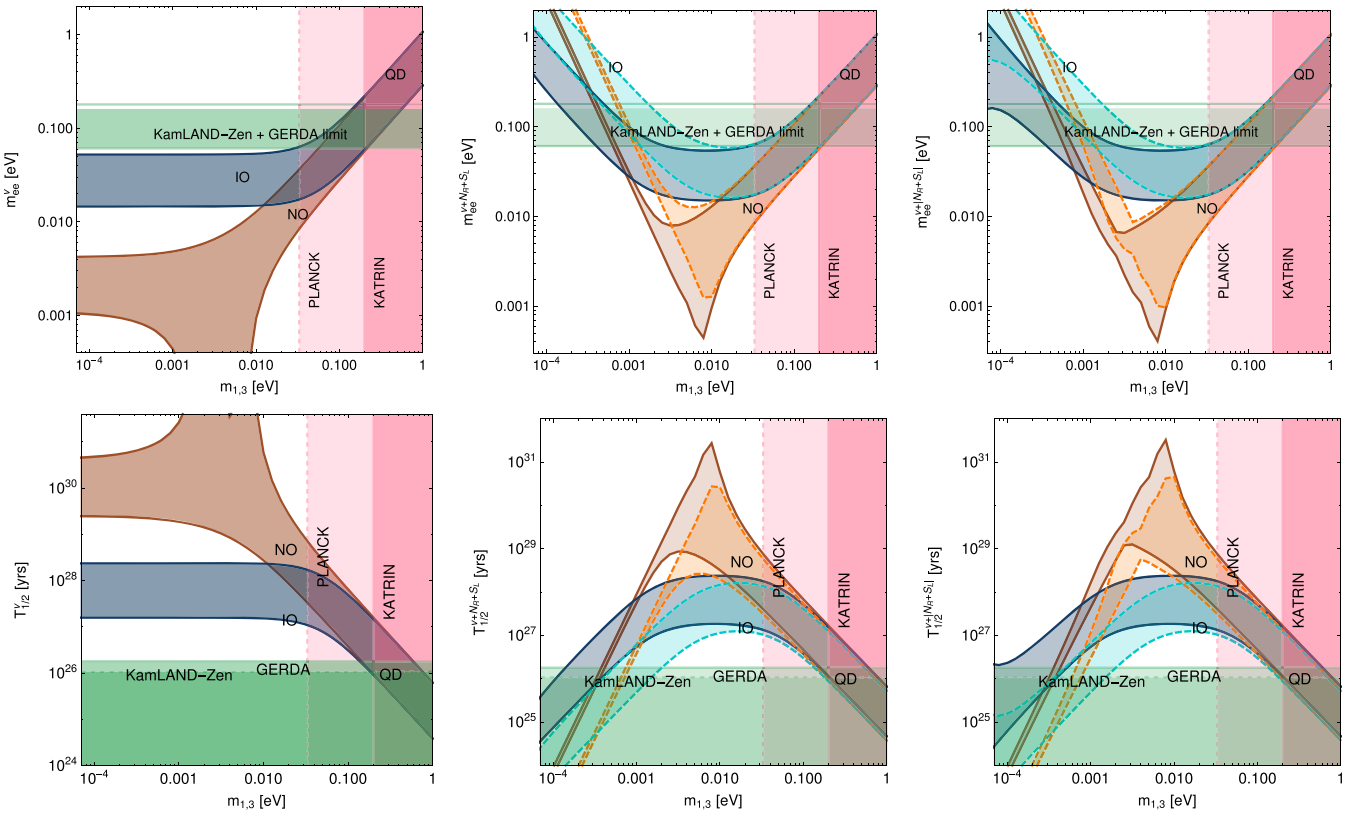

FIG. 4. Plots showing effective Majorana mass parameter (upper panel) and half-life (lower panel) of $0\nu\beta\beta$ decay as functions of the lightest neutrino mass $m_{1(3)}$ in the case of NO (IO) light neutrino mass spectrum. The left-upper panel shows the dependence on $m_{1(3)}$ of the standard mechanism effective Majorana mass, while in the middle- and right-upper panels, the dependence of the generalized effective Majorana mass in which the contributions due to the exchange of the heavy Majorana fermions $N_{1,2,3}$ and $S_{1,2,3}$ are included without accounting for (middle-upper panel) and accounting for (upper-right panel) their interference. The brown and blue bands correspond respectively to the NO (NH) and IO (IH) types of light neutrino mass spectrum. The overlap of the two bands indicates the region of the QD spectrum. The lower panels show the dependence on $m_{1(3)}$ of the $0\nu\beta\beta$ decay half-lives corresponding to the respective upper panels. The green horizontal band represents the current bound on effective Majorana mass from the experiments KamLAND-Zen and GERDA as given in Table IV, whereas the vertical pink bands represent the bound corresponding to the upper limit on the sum of light neutrino masses of 0.12 eV reported by the Planck [19] and the prospective bound of 0.20 eV that can be set by the KATRIN [129] experiment. See text for further details.

fermions $N_{1,2,3}$ and $S_{1,2,3}$ are included without accounting for (middle panel) and accounting for (right panel) their interference. The brown and blue bands correspond respectively to the NO (NH) and IO (IH) types of light neutrino mass spectrum. The overlap of the two bands indicates the region of the QD spectrum. Following the discussion of NME in Sec. IV, the ratio of nuclear matrix elements $\mathcal{M}_N^{0\nu}/\mathcal{M}_\nu^{0\nu}$ is varied in the interval 22.2–76.3, as given in Eq. (4.7). The minimal (maximal) value in this interval, $\mathcal{M}_N^{0\nu}/\mathcal{M}_\nu^{0\nu} = 22.2(76.3)$, corresponds to $\mathcal{M}_\nu^{0\nu} = 4.68(5.26)$. The results for $\mathcal{M}_N^{0\nu}/\mathcal{M}_\nu^{0\nu} = 22.2(76.3)$ are indicated with solid (dashed) lines. For the parameters M_{W_R}, $m_{N_{1(3)}}$ and $m_{S_{3(2)}}$ the reference values of 5.5 TeV, 300 GeV, and 3 TeV, respectively, are used. All plots are obtained by varying the neutrino oscillation parameters in their respective 3σ allowed ranges. The Majorana phases α and β are varied in the interval $[0, \pi]$, while the Dirac phase δ is set to zero. For both $\mathcal{M}_N^{0\nu}/\mathcal{M}_\nu^{0\nu} = 22.2$ and 76.3, the curves showing the maximal (minimal) values of GEMM as functions of $m_{1(3)}$ correspond to $\alpha = \beta = 0$ ($\alpha = \pi$, $\beta = 0$). The lower panels show the dependence on $m_{1(3)}$ of the $0\nu\beta\beta$ decay half-lives corresponding to the respective upper panels. The green horizontal band represents the current bound on effective Majorana mass from the experiments KamLAND-Zen and GERDA as given in Table IV, whereas the vertical pink bands represent the bound corresponding to the upper limit on the sum of light neutrino masses of 0.12 eV reported by the Planck experiment [19] and the prospective bound of 0.20 eV that can be set by the KATRIN [129] experiment.

A comparison between the upper left and right panels in Fig. 4 shows that the presence of the new

nonstandard contributions change drastically the dependence of the effective Majorana mass of the standard mechanism $|m^{\nu}_{ee}|$ on the lightest neutrino mass $m_{1(3)}$ at $m_{1(3)} < 10^{-2}$ eV, where the new contributions dominate over the standard contribution. At $m_{1(3)} \gtrsim 10^{-2}$ eV the new contributions are strongly suppressed and practically negligible and we have $|m^{\nu+|N+S|}_{ee}| \cong |m^{\nu}_{ee}|$, as also is clearly seen in Fig. 4.

The nonstandard contributions are so large at relatively small values of the $m_{1(3)}$ that for $m_{1(3)} \lesssim 2 \times 10^{-4}$ eV in the NO case they are ruled out even for the minimal value of $M^{N}_{0\nu}/M^{\nu}_{0\nu} = 22.2$ by the existing upper limits from the KamLAND-Zen and GERDA experiments. In the IO case the new contributions are also ruled our for $M^{N}_{0\nu}/M^{\nu}_{0\nu} = 76.3$; for $M^{N}_{0\nu}/M^{\nu}_{0\nu} = 22.2$ they are ruled out for $\alpha = \beta = 0$, while for $\alpha = \pi$, $\beta = 0$, they are compatible with the KamLAND-Zen and GERDA upper limits.

For NO spectrum and $\alpha = \beta = 0$, the inequality $|m^{\nu+|N+S|}_{ee}| > (\gg)|m^{\nu}_{ee}|$ always holds in the interval of values of $m_1 \cong (3 \times 10^{-4} - 8 \times 10^{-3})$ eV where the nonstandard contributions are significant. In this interval and for $M^{N}_{0\nu}/M^{\nu}_{0\nu} = 76.3(22.2)$, $|m^{\nu+|N+S|}_{ee}| \gtrsim 0.009$ (0.007) eV, and with the exception of a very narrow interval around $m_1 \cong 4.0(2.5) \times 10^{-3}$ eV at which the quoted minimum of $|m^{\nu+|N+S|}_{ee}|$ takes place, we have $|m^{\nu+|N+S|}_{ee}| \gtrsim 0.010$ eV. In most of the considered intervals of values of m_1 the half-life $T^{\nu+|N_R+S_L|}_{1/2} \lesssim 10^{28}$ yrs.

In the case of NO spectrum, $\alpha = \pi, \beta = 0$ and $M^{N}_{0\nu}/M^{\nu}_{0\nu} = 76.3(22.2)$, the value of $|m^{\nu+|N+S|}_{ee}| \gtrsim 0.010$ eV, and $T^{\nu+|N_R+S_L|}_{1/2} \lesssim 10^{28}$ yrs, at $m_1 \lesssim 2.0(1.5) \times 10^{-3}$ eV. For the minimal value of $|m^{\nu+|N+S|}_{ee}|$ we find $\min(|m^{\nu+|N+S|}_{ee}|) \cong 9(3) \times 10^{-4}$ eV. It takes place at $m_1 \cong 9.0(8.0) \times 10^{-3}$ eV. We recall that $|m^{\nu}_{ee}|$ goes through zero at $m_1 \cong 2.26 \times 10^{-3}$ eV, while $|m^{\nu+|N+S|}_{ee}| \cong 18.3(5.3) \times 10^{-3}$ eV at this value of m_1.

For the IO spectrum, we have $|m^{\nu+|N+S|}_{ee}| \gtrsim 0.015$ eV for $m_3 < 9 \times 10^{-3}$ eV, where $|m^{\nu+|N+S|}_{ee}| > |m^{\nu}_{ee}|$ for any of the considered values of $M^{N}_{0\nu}/M^{\nu}_{0\nu}$ and of α and β. The approximate equality $|m^{\nu+|N+S|}_{ee}| \cong |m^{\nu}_{ee}|$ holds at $m_3 \gtrsim 10^{-2}$ eV. For all considered values of m_3, $M^{N}_{0\nu}/M^{\nu}_{0\nu}$ and the Majorana phases the predicted half-life $T^{\nu+|N_R+S_L|}_{1/2} \lesssim 10^{28}$ yrs, while in the case of $\alpha = \beta = 0$, we have $T^{\nu+|N_R+S_L|}_{1/2} \lesssim 2 \times 10^{27}$ yrs.

It follows from our numerical analysis that most of the parameter space of the considered model, the predictions for the $0\nu\beta\beta$ decay generalized effective Majorana mass and half-life are within the sensitivity range of the planned next generation of neutrinoless double beta decay LEGEND-200 (LEGEND-1000), nEXO, KamlAND-Zen-II, CUPID, NEXT-HD (see [130,131] and references quoted therein).

VI. COMMENTS ON LFV AND LHC SIGNATURES

The considered model has rich lepton flavor violating (LFV) and collider phenomenology. A detailed investigation of the model's phenomenology is beyond the scope of the present study. We limit ourselves here with a few brief comments.

The LFV processes as like $\mu \to e + \gamma$, $\mu \to 3e$ decays and $\mu - e$ conversion in nuclei can be mediated by heavy RH and sterile neutrinos $N_{1,2,3}$ and $S_{1,2,3}$. Although we expect the contributions due to $N_{1,2,3}$ and especially due to $S_{1,2,3}$ to be rather suppressed, there might be a relatively large region of the model's parameter space where they might still be in the range of sensitivity of the next generation of experiments MEG II, Mu3e, Mu2e, COMET, and PRISM/PRIME (see e.g., [132] and the references therein).

At LHC, the main channel for the production of the heavy RH neutrinos $N_{1,2,3}$ is via on-shell Z_R production and W_R fusion and can be expressed as $p + p \to W^{\pm}_R \to l^{\pm} + N_j$, $l = e, \mu, \tau$. This N_j further decays as $N_j \to W^{*}_R \to l'^{\pm} + 2j$, $l' = e, \mu, \tau$, which is considered as the "smoking gun" signature of lepton number and lepton flavor violation at LHC. This rapid decay of N_j happens in the case its mass is sufficiently large. Our model satisfies this requirement as we have taken $\max(M_{N_j}) \sim 100$ GeV. We recall that the mass of W_R is constrained by experiments CMS, ATLAS and low energy precision measurements as $M_{W_R} \gtrsim 5$ TeV [91–95] and considering the relation $M_{Z_R} \simeq 1.2 M_{W_R}$, the mass of Z_R can be constrained as $M_{Z_R} \gtrsim 6$ TeV. If the mass of N_j lies in the range 5–20 GeV, then it takes some time to decay and travels some distance resulting in a displaced vertex of leptons [133,134]. So, the observable in this case would be a prompt charged lepton and a displaced leptonic vertex. The current status of displaced vertex searches at LHC can be found in Ref. [135–137]. Another distinguishing feature in the signatures of small mass (<100 GeV) and large mass (~800 GeV) RH neutrinos N_j is the angle between the produced charged leptons. In the former case, parallel tracks of charged leptons are expected, whereas in the later case, back-to-back emissions are expected [138].

VII. SUMMARY

In the present article, we have derived predictions for the neutrinoless double beta ($0\nu\beta\beta$) decay generalized effective Majorana mass and half-life in a left-right (L-R) symmetric model with the double seesaw mechanism at the TeV scale. The gauge group of the model is the standard L-R symmetric extension of the Standard Model (SM) gauge group: $\mathcal{G}_{LR} \equiv SU(2)_L \times SU(2)_R \times U(1)_{B-L}$. The fermion

sector has the usual for the L-R symmetric models, three families of left-handed and right-handed quark and lepton fields, including right-handed neutrino fields $N_{\beta R}, \beta = e, \mu, \tau$, assigned respectively to $SU(2)_L$ and $SU(2)_R$ doublets. It included also three $SU(2)_{L,R}$ singlet LH fermion fields $S_{\gamma L}$. The Higgs sector is composed of two $SU(2)_L$ and $SU(2)_R$ Higgs doublets H_L and H_R, and of a bidoublet Φ. The vacuum expectation value (VEV) of the $SU(2)_R$ Higgs doublet H_R breaks the $\mathcal{G}_{LR}$ gauge symmetry to the SM gauge symmetry $SU(2)_L \times U(1)_Y$, while the VEVs of the two neutral components of the bidoublet Φ break $SU(2)_L \times U(1)_Y$ to $U(1)_{\rm em}$. The Yukawa couplings of the LH and RH fermion doublets to the bidoublet Φ generate (via the VEVs of the neutral components of Φ) Dirac mass terms for the quarks and charged leptons, as well as a $\nu_{\alpha L} - N_{\beta R}$ Dirac mass term $M^{\nu}_{\rm D}$ involving the LH active flavor neutrino fields $\nu_{\alpha L}$ and the RH fields $N_{\beta R}, \alpha, \beta = e, \mu, \tau$. The singlet LH fermion fields $S_{\gamma L}$ are assumed to have a Majorana mass term $M_{\rm S}$ and Yukawa coupling with the RH doublets containing $N_{\beta R}$ which involves H_R. This Yukawa coupling produces a $S_{\gamma L} - N_{\beta R}$ Dirac mass term $M_{\rm RS}$ when H_R develops a nonzero VEV. Under the condition $|M_{\rm RS}| \ll |M_{\rm S}|$, the RH neutrinos $N_{\beta R}$ get a Majorana mass term $M_{\rm R} \cong -M_{\rm RS} M_{\rm S}^{-1} M_{\rm RS}^{T}$ via a seesaw-like mechanism. This in turn generates a Majorana mass term for the LH flavor neutrinos $m_\nu \cong -M^{\nu}_{\rm D} M_{\rm R}^{-1} (M^{\nu}_{\rm D})^{T}$ via a second seesaw mechanism.[2] In such a way, the model contains in addition to the three light Majorana neutrinos ν_i having masses m_i, two sets of heavy Majorana particles N_j and S_k, $j, k = 1, 2, 3$, with masses $m_{N_j} \ll m_{S_k}$. The double seesaw scenario allows the RH neutrinos N_j to have masses naturally at the GeV–TeV scale.

In our analysis of the $0\nu\beta\beta$ decay predictions of the model, we have considered the case of $m_{N_j} \sim (1 - 1000)$ GeV and $\max(m_{S_k}) \sim (1 - 10)$ TeV, $m_{N_j} \ll m_{S_k}$. Working with a specific version of the model which can be obtained by employing symmetry arguments and in which the Dirac mass terms $M^{\nu}_{\rm D}$ and $M_{\rm RS}$ are diagonal, $M^{\nu}_{\rm D} = k_d \mathbf{I}$, $M_{\rm RS} = k_{rs} \mathbf{I}$, k_d, and k_{RS} being constant mass parameters and $\mathbf{I}$ the 3×3 unit matrix, we have studied in detail the new "nonstandard" contributions to the $0\nu\beta\beta$ decay amplitude and half-life arising from diagrams with an exchange of virtual N_j and S_k. The self-consistency of the considered setup requires that the lightest neutrino mass for the neutrino mass spectrum with normal ordering (NO), m_1, or with inverted ordering (IO), m_3, has to be not smaller that approximately 10^{-4} eV. Moreover, the RH neutrino ($N_{\beta R}$) and sterile fermion ($S_{\gamma L}$) mixings are determined by the light neutrino PMNS mixing matrix. In the analysis of the new nonstandard contributions to the $0\nu\beta\beta$ decay amplitude we took into account the values of the nuclear matrix elements $\mathcal{M}^{0\nu}_{N}$ and $\mathcal{M}^{0\nu}_{\nu}$ associated with, respectively, the light and heavy Majorana neutrino exchange contributions, calculated for the four isotopes ^{76}Ge, ^{82}Se, ^{130}Te, and ^{136}Xe by six different groups of authors using different methods of NME calculation (Table III). We made use of the fact that the ratio $\mathcal{M}^{0\nu}_{N}/\mathcal{M}^{0\nu}_{\nu}$ reported by each of the six cited groups is essentially the same for the considered four isotopes—it varies with the isotope by not more than ∼15%. For a given isotope the ratio of interest obtained by the six different methods of NME calculation varies by a factor of up to ∼3.5. In view of this, we took into account the uncertainties in the NME calculations by using the following reference range of the ratio $\mathcal{M}^{0\nu}_{N}/\mathcal{M}^{0\nu}_{\nu} = 22.2$–$76.3$, which corresponds to ^{76}Ge.

We analyzed in detail the properties of the new nonstandard contributions to the $0\nu\beta\beta$ decay amplitude arising due to the exchange of virtual heavy Majorana fermions N_j and S_k, parametrized as effective Majorana masses $m^{N}_{\beta\beta,R}$ Eq. (5.3) and $m^{S}_{\beta\beta,R}$ Eq. (5.7), respectively. These analyses showed that both $|m^{N}_{\beta\beta,R}|$ and $|m^{S}_{\beta\beta,R}|$ are strongly enhanced at relatively small values of the lightest neutrino mass $m_{1(3)} \sim (10^{-4} - 8 \times 10^{-3})$ eV. The effect of this enhancement is particularly important in the case of NO neutrino mass spectrum. The nonstandard contributions are so large at the indicated small values of $m_{1(3)}$ that for $m_1 \lesssim 2 \times 10^{-4}$ eV in the NO case, they are strongly disfavored (if not ruled out) even for the minimal value of $M^{N}_{0\nu}/M^{\nu}_{0\nu} = 22.2$ by the existing upper limits from the KamLAND-Zen and GERDA experiments. In the IO case, the new contributions are also strongly disfavored for $M^{N}_{0\nu}/M^{\nu}_{0\nu} = 76.3$; for $M^{N}_{0\nu}/M^{\nu}_{0\nu} = 22.2$ they are disfavored for $\alpha = \beta = 0$, while for $\alpha = \pi$, $\beta = 0$, they are still compatible with the KamLAND-Zen and GERDA conservative upper limits. We find, in general, that in both NO and IO cases the new nonstandard contributions due to N_j and S_k exchange are dominant over the standard light neutrino exchange contribution at values of the lightest neutrino mass $m_{1(3)} \sim (10^{-4}$–$10^{-2})$ eV: $|m^{\nu+|N+S|}_{ee}| > (\gg)|m^{\nu}_{ee}|$, where $m^{\nu+|N+S|}_{ee}$ is the generalized effective Majorana mass (GEMM) which accounts for all contributions to the $0\nu\beta\beta$ decay amplitude [Eqs. (4.12), (4.13), and (4.15)], and m^{ν}_{ee} is the effective Majorana mass associated with the standard light neutrino exchange contribution [Eq. (4.16)]. The effective Majorana mass $|m^{S}_{\beta\beta,R}|$ associated with S_k exchange contribution was shown to be practically independent of the Majorana phases α and β, while that due to exchange of N_j, $|m^{N}_{\beta\beta,R}|$, exhibits strong dependence on α and β similar to $|m^{\nu}_{ee}|$.

For NO spectrum and $\alpha = \beta = 0$, the inequality $|m^{\nu+|N+S|}_{ee}| > (\gg)|m^{\nu}_{ee}|$ always holds in the interval of

[2]Hence the term "double or cascade seesaw mechanism of neutrino mass generation."

values of 10^{-4} eV $\lesssim m_1 \lesssim 8 \times 10^{-3}$ eV where the nonstandard contributions are significant. In this interval and for $M^N_{0\nu}/M^\nu_{0\nu} = 76.3(22.2)$, $|m^{\nu+|N+S|}_{ee}| \gtrsim 0.009(0.007)$ eV. With the exception of a very narrow interval around $m_1 \cong 4.0(2.5) \times 10^{-3}$ eV at which the quoted minimum of $|m^{\nu+|N+S|}_{ee}|$ takes place, we have $|m^{\nu+|N+S|}_{ee}| \gtrsim 0.010$ eV. In most of the considered intervals of values of m_1 the $0\nu\beta\beta$ decay half-life $T^{\nu+|N_R+S_L|}_{1/2} \lesssim 10^{28}$ yrs.

In the case of NO spectrum, $\alpha = \pi$, $\beta = 0$ and $M^N_{0\nu}/M^\nu_{0\nu} = 76.3(22.2)$, we find that $|m^{\nu+|N+S|}_{ee}| \gtrsim 0.010$ eV, and $T^{\nu+|N_R+S_L|}_{1/2} \lesssim 10^{28}$ yrs, at $m_1 \lesssim 2.0(1.5) \times 10^{-3}$ eV. For the minimal value of $|m^{\nu+|N+S|}_{ee}|$ we get $\min(|m^{\nu+|N+S|}_{ee}|) \cong 9(3) \times 10^{-4}$ eV. It takes place at $m_1 \cong 9.0(8.0) \times 10^{-3}$ eV. We note that $|m^\nu_{ee}|$ goes through zero at $m_1 \cong 2.26 \times 10^{-3}$ eV, while $|m^{\nu+|N+S|}_{ee}| \cong 18.8(5.3) \times 10^{-3}$ eV at this value of m_1. Thus, the strong suppression of the $0\nu\beta\beta$ decay rate at $m_1 \sim 2.26 \times 10^{-3}$ eV and in the interval $m_1 \cong (1.5\text{–}8.0) \times 10^{-3}$ eV in the case of only standard contribution due to the exchange of light Majorana neutrinos ν_i (Fig. 4, upper left panel) is avoided due to the new nonstandard contributions.

For the IO spectrum, we find that $|m^{\nu+|N+S|}_{ee}| \gtrsim 0.015$ eV for $m_3 < 9 \times 10^{-3}$ eV, where $|m^{\nu+|N+S|}_{ee}| > |m^\nu_{ee}|$ for any of the considered values of $M^N_{0\nu}/M^\nu_{0\nu}$ and of α and β. The approximate equality $|m^{\nu+|N+S|}_{ee}| \cong |m^\nu_{ee}|$ holds at $m_3 \gtrsim 10^{-2}$ eV. For all considered values of the parameters the predicted half-life $T^{\nu+|N_R+S_L|}_{1/2} \lesssim 10^{28}$ yrs, while in the case of $\alpha = \beta = 0$, we have $T^{\nu+|N_R+S_L|}_{1/2} \lesssim 2 \times 10^{27}$ yrs.

It follows from our results that in most of the parameter space of the considered model, the predictions for the $0\nu\beta\beta$ decay generalized effective Majorana mass and half-life are within the sensitivity range of the planned next generation of neutrinoless double beta decay experiments LEGEND-200 (LEGEND-1000), nEXO, KamlAND-Zen-II, CUPID, and NEXT-HD (see [130,131] and references quoted therein).

ACKNOWLEDGMENTS

Purushottam Sahu would like to acknowledge the Ministry of Education, Government of India for financial support. P. S. also acknowledges the support from the Abdus Salam International Centre for Theoretical Physics (ICTP) under the "ICTP Sandwich Training Educational Programme (STEP)" SMR.3676 and SMR.3799. The work of S. T. P. was supported in part by the European Union's Horizon 2020 research and innovation program under the Marie Skłodowska-Curie Grant Agreement No. 860881-HIDDeN, by the Italian INFN program on Theoretical Astroparticle Physics and by the World Premier International Research Center Initiative (WPI Initiative, MEXT), Japan. S. T. P. would like to thank Kavli IPMU, University of Tokyo, where part of this study was performed for the kind hospitality.

APPENDIX: DERIVATION OF NEUTRINO MASSES AND MIXINGS IN LEFT-RIGHT DOUBLE SEESAW MODEL

A. LRDSM mass matrix

We discuss here the implementation and derivation of double seesaw mechanism in the considered left-right symmetric model. The neutral fermions needed for the left-right double seesaw model (LRDSM) are active left-handed neutrinos, ν_L, active right-handed neutrinos, N_R and sterile neutrinos, S_L. The relevant mass terms are given by

$$\begin{aligned}
\mathcal{L}_{\rm LRDSM} &= \mathcal{L}_{M_D} + \mathcal{L}_{M_{RS}} + \mathcal{L}_{M_S},\\
\mathcal{L}_{M_D} &= -\sum_{\alpha,\beta} \overline{\nu_{\alpha L}} [M_D]_{\alpha\beta} N_{\beta R} + \text{H.c.},\\
\mathcal{L}_{M_{RS}} &= \sum_{\alpha,\beta} \overline{S_{\alpha L}} [M_{RS}]_{\alpha\beta} N_{\beta R} + \text{H.c.},\\
\mathcal{L}_{M_S} &= \frac{1}{2} \sum_{\alpha,\beta} \overline{S^c_{\alpha L}} [M_S]_{\alpha\beta} S_{\beta L} + \text{H.c.}
\end{aligned} \tag{A1}$$

The flavor states for active left-handed neutrinos $\nu_{\alpha L}$, right-handed neutrinos $N_{\beta R}$ and sterile neutrinos $S_{\gamma L}$ are defined as follows:

$$\nu_{\alpha L} = \begin{pmatrix} \nu_{eL} \\ \nu_{\mu L} \\ \nu_{\tau L} \end{pmatrix}, \quad N_{\beta R} = \begin{pmatrix} N_{1R} \\ N_{2R} \\ N_{3R} \end{pmatrix}, \quad S_{\gamma L} = \begin{pmatrix} S_{1L} \\ S_{2L} \\ S_{3L} \end{pmatrix}. \tag{A2}$$

Similarly, their mass states can be written as

$$\nu_{iL} = \begin{pmatrix} \nu_{1L} \\ \nu_{2L} \\ \nu_{3L} \end{pmatrix}, \quad N^c_{jR} = \begin{pmatrix} N^c_{1R} \\ N^c_{2R} \\ N^c_{3R} \end{pmatrix}, \quad S_{kL} = \begin{pmatrix} S_{1L} \\ S_{2L} \\ S_{3L} \end{pmatrix}. \tag{A3}$$

The 9×9 neutral lepton mass matrix in the basis (ν_L, N^c_R, S_L) is given by

$$\mathcal{M}_{LRDSM} = \left[\begin{array}{ccc|c} \mathbf{0} & M_D & & 0 \\ M^T_D & \mathbf{0} & & M_{RS} \\ \hline 0 & M^T_{RS} & & M_S \end{array}\right], \tag{A4}$$

where each elements of the matrix is a 3×3 matrix. Here M_D is the Dirac neutrino mass matrix connecting $\nu_L - N_R$,

M_{RS} is the mixing matrix in the $N_R - S_L$ sector, M_S is the Majorana mass matrix for sterile neutrino S_L.

In order to diagonalize the above mass matrix we have used the following mass hierarchy,

$$M_D < M_{RS} < M_S. \tag{A5}$$

The diagonalization of $\mathcal{M}_{\rm LRDSM}$ after changing it from flavor basis to mass basis is done by a generalized unitary transformation as

$$|\Psi\rangle_{\rm flavor} = V|\Psi\rangle_{\rm mass} \tag{A6}$$

$$\text{or,} \begin{pmatrix} \nu_{\alpha L} \\ N^c_{\beta R} \\ S_{\gamma L} \end{pmatrix} = \begin{pmatrix} V^{\nu\nu}_{\alpha i} & V^{\nu N}_{\alpha j} & V^{\nu S}_{\alpha k} \\ V^{N\nu}_{\beta i} & V^{NN}_{\beta j} & V^{NS}_{\beta k} \\ V^{S\nu}_{\gamma i} & V^{SN}_{\gamma j} & V^{SS}_{\gamma k} \end{pmatrix} \begin{pmatrix} \nu_i \\ N^c_j \\ S_k \end{pmatrix} \tag{A7}$$

$$\begin{aligned} V^\dagger \mathcal{M}_{\rm LRDSM} V^* &= \hat{\mathcal{M}}_{\rm LRDSM} \\ &= \text{diag}(m_i, m_{N_j}, m_{S_k}) \\ &= \text{diag}(m_1, m_2, m_3, m_{N_1}, m_{N_2}, m_{N_3}, \\ &\quad m_{S_1}, m_{S_2}, m_{S_3}). \end{aligned} \tag{A8}$$

Here the indices α, β, γ run over three generations of light left-handed neutrinos, heavy right-handed neutrinos and sterile neutrinos respectively, whereas the indices i, j, k run over corresponding mass states.

B. Block diagonalization of double seesaw mass matrix in LRDSM

Let us write the matrix in Eq. (A4) as

$$\begin{aligned} \mathcal{M}_{LRDSM} = \mathcal{M}_\nu &= \begin{pmatrix} \mathcal{M}_L & \mathcal{M}_D \\ \mathcal{M}_D^T & \mathcal{M}_S \end{pmatrix}, \quad \text{where} \\ \mathcal{M}_L &= \begin{pmatrix} 0 & M_D \\ M_D^T & 0 \end{pmatrix}, \qquad \mathcal{M}_D = \begin{pmatrix} 0 \\ M_{RS} \end{pmatrix}, \\ \mathcal{M}_S &= M_S. \end{aligned} \tag{A9}$$

The complete block diagonalization is achieved in two steps by recursively integrating out the heavier modes as

$$\mathcal{W}_1^\dagger \mathcal{M}_\nu \mathcal{W}_1^* = \hat{\mathcal{M}}'_\nu \quad \text{and} \quad \mathcal{W}_2^\dagger \hat{\mathcal{M}}'_\nu \mathcal{W}_2^* = \hat{\mathcal{M}}_\nu, \tag{A10}$$

where $\hat{\mathcal{M}}'_\nu$ is block diagonalized 9×9 matrix after integrating out the heaviest mode and $\hat{\mathcal{M}}_\nu$ is the block diagonalized 9×9 matrix after integrating out the next heaviest mode. The transformation matrix $\mathcal{W}_1$ can be written as a general unitary matrix in the form

$$\mathcal{W}_1^* = \begin{pmatrix} \sqrt{1 - \mathcal{B}\mathcal{B}^\dagger} & \mathcal{B} \\ -\mathcal{B}^\dagger & \sqrt{1 - \mathcal{B}^\dagger \mathcal{B}} \end{pmatrix}, \tag{A11}$$

where $\mathcal{B}$ is a 6×3 dimensional matrix,

$$\begin{aligned} \sqrt{1 - \mathcal{B}\mathcal{B}^\dagger} &= 1 - \frac{1}{2}\mathcal{B}\mathcal{B}^\dagger - \frac{1}{8}(\mathcal{B}\mathcal{B}^\dagger)^2 + \cdots \\ \mathcal{B} &= \sum \mathcal{B}_i. \end{aligned} \tag{A12}$$

At leading order it looks like

$$\sqrt{1 - \mathcal{B}\mathcal{B}^\dagger} \simeq 1 - \frac{1}{2}\mathcal{B}\mathcal{B}^\dagger - \frac{1}{8}(\mathcal{B}_1\mathcal{B}_2^\dagger + \mathcal{B}_2\mathcal{B}_1^\dagger). \tag{A13}$$

The form of mixing matrix $\mathcal{B}_1^\dagger$ and $\mathcal{B}_1$ is given by

$$\begin{aligned} \mathcal{B}_1^\dagger &= \mathcal{M}_S^{-1} \cdot \mathcal{M}_D^T = M_S^{-1} \cdot \begin{pmatrix} 0 & M_{RS}^T \end{pmatrix} \\ &= \begin{pmatrix} 0 & M_S^{-1} \cdot M_{RS}^T \end{pmatrix}, \\ \mathcal{B}_1 &= \begin{pmatrix} 0 \\ M_{RS} M_S^{-1} \end{pmatrix}, \\ \sqrt{1 - \mathcal{B}\mathcal{B}^\dagger} &\simeq \begin{pmatrix} 1 & 0 \\ 0 & 1 - \frac{1}{2} M_{RS} M_S^{-1} \cdot M_S^{-1} M_{RS}^T \end{pmatrix}, \\ \sqrt{1 - \mathcal{B}^\dagger \mathcal{B}} &\simeq 1 - \frac{1}{2} M_S^{-1} M_{RS}^T \cdot M_{RS} M_S^{-1}. \end{aligned} \tag{A14}$$

Thus, the first block-diagonalized mixing matrix $\mathcal{W}_1$ becomes

$$\mathcal{W}_1 = \begin{pmatrix} 1 & 0 & 0 \\ 0 & 1 - \frac{1}{2} M_{RS} M_S^{-1} \cdot M_S^{-1} M_{RS}^T & M_{RS} M_S^{-1} \\ 0 & -M_S^{-1} M_{RS}^T & 1 - \frac{1}{2} M_S^{-1} M_{RS}^T \cdot M_{RS} M_S^{-1} \end{pmatrix}. \tag{A15}$$

After this diagonalization, $\hat{\mathcal{M}}'_\nu$ has the following form:

$$\hat{\mathcal{M}}'_\nu = \begin{pmatrix} \mathcal{M}_{\rm eff} & 0 \\ 0 & \mathcal{M}_S \end{pmatrix}, \tag{A16}$$

where

$$\begin{aligned}\mathcal{M}_{\text{eff}} &= \mathcal{M}_L - \mathcal{M}_D\mathcal{M}_S^{-1}\mathcal{M}_D^T \\ &= \begin{pmatrix} 0 & M_D \\ M_D^T & 0 \end{pmatrix} - \begin{pmatrix} 0 \\ M_{RS} \end{pmatrix} M_S^{-1} \begin{pmatrix} 0 & M_{RS}^T \end{pmatrix} \\ &= \begin{pmatrix} 0 & M_D \\ M_D^T & -M_{RS}M_S^{-1}M_{RS}^T \end{pmatrix}. \end{aligned} \tag{A17}$$

$\mathcal{M}_{\text{eff}}$ can be further diagonalized by $\mathcal{W}_2$ as

$$\mathcal{S}^\dagger \mathcal{M}_{\text{eff}} \mathcal{S}^* = \begin{pmatrix} m_\nu & 0 \\ 0 & M_R \end{pmatrix}, \tag{A18}$$

where

$$\begin{aligned} m_\nu &= -M_D(-M_{RS}M_S^{-1}M_{RS}^T)^{-1}M_D^T, \\ M_R &= -M_{RS}M_S^{-1}M_{RS}^T. \end{aligned} \tag{A19}$$

The transformation matrix $\mathcal{S}$ is

$$\mathcal{S}^* = \begin{pmatrix} \sqrt{1-\mathcal{A}\mathcal{A}^\dagger} & \mathcal{A} \\ -\mathcal{A}^\dagger & \sqrt{1-\mathcal{A}^\dagger\mathcal{A}} \end{pmatrix} \tag{A20}$$

such that

$$\mathcal{A}^\dagger = (-M_{RS}M_S^{-1}M_{RS}^T)^{-1}M_D, \tag{A21}$$

$$= -M_{RS}^{-1^T} M_S M_{RS}^{-1} M_D = X^\dagger. \tag{A22}$$

Thus,

$$\mathcal{W}_2 = \begin{pmatrix} \mathcal{S} & 0 \\ 0 & 1 \end{pmatrix} \tag{A23}$$

$$= \begin{pmatrix} 1-\frac{1}{2}XX^\dagger & X & 0 \\ -X^\dagger & 1-\frac{1}{2}X^\dagger X & 0 \\ 0 & 0 & 1 \end{pmatrix}. \tag{A24}$$

C. Complete diagonalization and physical neutrino masses

After block diagonalization, the mass matrix for the three types of neutrinos are further diagonalized by respective unitary mixing matrices U_ν, U_N, U_S resulting in physical masses for the neutrinos as follows:

$$U_{9\times9} = \begin{pmatrix} U_{\nu 3\times3} & 0_{3\times3} & 0_{3\times3} \\ 0_{3\times3} & U_{N3\times3} & 0_{3\times3} \\ 0_{3\times3} & 0_{3\times3} & U_{S3\times3} \end{pmatrix}, \tag{A25}$$

$$\begin{aligned} U_\nu^\dagger m_\nu U_\nu^* &= \hat{m}_\nu = \text{diag}(m_{\nu_1}, m_{\nu_2}, m_{\nu_3}), \\ U_N^\dagger M_N U_N^* &= \hat{M}_N = \text{diag}(M_{N_1}, M_{N_2}, M_{N_3}), \\ U_S^\dagger M_S U_S^* &= \hat{M}_S = \text{diag}(M_{S_1}, M_{S_2}, M_{S_3}). \end{aligned} \tag{A26}$$

The complete mixing matrix now becomes

$$\begin{aligned} V &= \mathcal{W}_1 \cdot \mathcal{W}_2 \cdot \mathcal{U} \\ &= \begin{pmatrix} 1 & 0 & 0 \\ 0 & 1-\frac{1}{2}YY^\dagger & Y \\ 0 & -Y^\dagger & 1-\frac{1}{2}Y^\dagger Y \end{pmatrix} \cdot \begin{pmatrix} 1-\frac{1}{2}XX^\dagger & X & 0 \\ -X^\dagger & 1-\frac{1}{2}X^\dagger X & 0 \\ 0 & 0 & 1 \end{pmatrix} \cdot \begin{pmatrix} U_\nu & 0 & 0 \\ 0 & U_N & 0 \\ 0 & 0 & U_S \end{pmatrix} \\ &= \begin{pmatrix} U_\nu\left(1-\frac{1}{2}XX^\dagger\right) & U_N X & 0 \\ -U\nu X^\dagger\left(1-\frac{1}{2}YY^\dagger\right) & U_N\left(1-\frac{1}{2}X^\dagger X\right)\left(1-\frac{1}{2}YY^\dagger\right) & U_S Y \\ U\nu X^\dagger Y^\dagger & -U_N Y^\dagger & U_S\left(1-\frac{1}{2}Y^\dagger Y\right) \end{pmatrix}, \end{aligned} \tag{A27}$$

where $X^\dagger = -M_{RS}^{-1}M_S M_{RS}^{-1}M_D$, $Y = M_{RS}M_S^{-1}$ and fixing the typical magnitudes for $M_D \simeq 0.1$ MeV, $M_{RS} \simeq 1$ TeV, $M_S \simeq 10$ TeV, we get $X \simeq 10^{-6}$, $Y \simeq 0.1$. Since U_ν, U_N and U_S are of $\mathcal{O}(1)$, the matrix elements of $\mathcal{V}$ are approximated to be

$$\begin{pmatrix} \mathcal{V}_{\alpha i}^{\nu\nu} & \mathcal{V}_{\alpha j}^{\nu N} & \mathcal{V}_{\alpha k}^{\nu S} \\ \mathcal{V}_{\beta i}^{N\nu} & \mathcal{V}_{\beta j}^{NN} & \mathcal{V}_{\beta k}^{NS} \\ \mathcal{V}_{\gamma i}^{S\nu} & \mathcal{V}_{\gamma j}^{SN} & \mathcal{V}_{\gamma k}^{SS} \end{pmatrix} \simeq \begin{pmatrix} \mathcal{O}(1.0) & \mathcal{O}(10^{-6}) & 0 \\ \mathcal{O}(10^{-6}) & \mathcal{O}(1.0) & \mathcal{O}(0.1) \\ \mathcal{O}(10^{-7}) & \mathcal{O}(0.1) & \mathcal{O}(1.0) \end{pmatrix} \tag{A28}$$

which generates sizable contribution to neutrinoless double beta decay.

[1] Q. R. Ahmad *et al.* (SNO Collaboration), Direct Evidence for Neutrino Flavor Transformation from Neutral Current Interactions in the Sudbury Neutrino Observatory, Phys. Rev. Lett. **89**, 011301 (2002).

[2] K. Abe *et al.* (Super-Kamiokande Collaboration), Solar neutrino measurements in Super-Kamiokande-IV, Phys. Rev. D **94**, 052010 (2016).

[3] K. Abe *et al.* (T2K Collaboration), Search for light sterile neutrinos with the T2K far detector Super-Kamiokande at a baseline of 295 km, Phys. Rev. D **99**, 071103 (2019).

[4] F. P. An *et al.* (Daya Bay Collaboration), Observation of Electron-Antineutrino Disappearance at Daya Bay, Phys. Rev. Lett. **108**, 171803 (2012).

[5] Y. Abe *et al.* (Double Chooz Collaboration), Indication of Reactor $\bar{\nu}_e$ Disappearance in the Double Chooz Experiment, Phys. Rev. Lett. **108**, 131801 (2012).

[6] P. Minkowski, $\mu \to e\gamma$ at a rate of one out of 10^9 muon decays?, Phys. Lett. **67B**, 421 (1977).

[7] R. N. Mohapatra and G. Senjanovic, Neutrino Mass and Spontaneous Parity Nonconservation, Phys. Rev. Lett. **44**, 912 (1980).

[8] T. Yanagida, Horizontal symmetry and masses of neutrinos, Conf. Proc. C **7902131**, 95 (1979).

[9] M. Gell-Mann, P. Ramond, and R. Slansky, Complex spinors and unified theories, Conf. Proc. C **790927**, 315 (1979).

[10] M. Magg and C. Wetterich, Neutrino mass problem and gauge hierarchy, Phys. Lett. **94B**, 61 (1980).

[11] J. Schechter and J. W. F. Valle, Neutrino masses in $SU(2) \times U(1)$ theories, Phys. Rev. D **22**, 2227 (1980).

[12] T. P. Cheng and L.-F. Li, Neutrino masses, mixings and oscillations in $SU(2) \times U(1)$ models of electroweak interactions, Phys. Rev. D **22**, 2860 (1980).

[13] G. Lazarides, Q. Shafi, and C. Wetterich, Proton lifetime and fermion masses in an SO(10) model, Nucl. Phys. **B181**, 287 (1981).

[14] R. N. Mohapatra and G. Senjanović, Neutrino masses and mixings in gauge models with spontaneous parity violation, Phys. Rev. D **23**, 165 (1981).

[15] R. Foot, H. Lew, X. G. He, and G. C. Joshi, Seesaw neutrino masses induced by a triplet of leptons, Z. Phys. C **44**, 441 (1989).

[16] B. He, N. Okada, and Q. Shafi, 125 GeV Higgs, type III seesaw and gauge–Higgs unification, Phys. Lett. B **716**, 197 (2012).

[17] J. Schechter and J. W. F. Valle, Neutrinoless double-β decay in $SU(2) \times U(1)$ theories, Phys. Rev. D **25**, 2951 (1982).

[18] S. M. Bilenky, S. Pascoli, and S. T. Petcov, Majorana neutrinos, neutrino mass spectrum, *CP* violation and neutrinoless double beta decay. 1. The three neutrino mixing case, Phys. Rev. D **64**, 053010 (2001).

[19] N. Aghanim *et al.* (Planck Collaboration), Planck 2018 results. VI. Cosmological parameters, Astron. Astrophys. **641**; A6 (2020); **652**, C4(E) (2021).

[20] K. N. Abazajian *et al.*, Synergy between cosmological and laboratory searches in neutrino physics: A white paper, arXiv:2203.07377.

[21] S. Roy Choudhury and S. Hannestad, Updated results on neutrino mass and mass hierarchy from cosmology with Planck 2018 likelihoods, J. Cosmol. Astropart. Phys. 07 (2020) 037.

[22] S. Roy Choudhury and S. Choubey, Updated bounds on sum of neutrino masses in various cosmological scenarios, J. Cosmol. Astropart. Phys. 09 (2018) 017.

[23] M. Agostini *et al.* (GERDA Collaboration), Final Results of GERDA on the Search for Neutrinoless Double-β Decay, Phys. Rev. Lett. **125**, 252502 (2020).

[24] G. Anton *et al.* (EXO-200 Collaboration), Search for Neutrinoless Double-β Decay with the Complete EXO-200 Dataset, Phys. Rev. Lett. **123**, 161802 (2019).

[25] A. Gando *et al.* (KamLAND-Zen Collaboration), Search for Majorana Neutrinos near the Inverted Mass Hierarchy Region with KamLAND-Zen, Phys. Rev. Lett. **117**, 082503 (2016); **117**, 109903(A) (2016).

[26] S. Abe *et al.* (KamLAND-Zen Collaboration), First Search for the Majorana Nature of Neutrinos in the Inverted Mass Ordering Region with KamLAND-Zen, Phys. Rev. Lett. **130**, 051801 (2023).

[27] R. N. Mohapatra, Mechanism for Understanding Small Neutrino Mass in Superstring Theories, Phys. Rev. Lett. **56**, 561 (1986).

[28] R. N. Mohapatra and J. W. F. Valle, Neutrino mass and baryon-number nonconservation in superstring models, Phys. Rev. D **34**, 1642 (1986).

[29] R. Mohapatra and J. C. Pati, A natural left-right symmetry, Phys. Rev. D **11**, 2558 (1975).

[30] J. C. Pati and A. Salam, Lepton number as the fourth color, Phys. Rev. D **10**, 275 (1974).

[31] G. Senjanović and R. N. Mohapatra, Exact left-right symmetry and spontaneous violation of parity, Phys. Rev. D **12**, 1502 (1975).

[32] G. Senjanović, Spontaneous breakdown of parity in a class of gauge theories, Nucl. Phys. **B153**, 334 (1979).

[33] W.-Y. Keung and G. Senjanović, Majorana Neutrinos and the Production of the Right-handed Charged Gauge Boson, Phys. Rev. Lett. **50**, 1427 (1983).

[34] A. Ferrari, J. Collot, M.-L. Andrieux, B. Belhorma, P. de Saintignon, J.-Y. Hostachy, P. Martin, and M. Wielers, Sensitivity study for new gauge bosons and right-handed Majorana neutrinos in pp collisions at $s = 14$-TeV, Phys. Rev. D **62**, 013001 (2000).

[35] M. Schmaltz and C. Spethmann, Two simple W' models for the early LHC, J. High Energy Phys. 07 (2011) 046.

[36] M. Nemevsek, F. Nesti, G. Senjanovic, and Y. Zhang, First limits on left-right symmetry scale from LHC data, Phys. Rev. D **83**, 115014 (2011).

[37] C.-Y. Chen and P. S. B. Dev, Multi-lepton collider signatures of heavy Dirac and Majorana neutrinos, Phys. Rev. D **85**, 093018 (2012).

[38] J. Chakrabortty, J. Gluza, R. Sevillano, and R. Szafron, Left-right symmetry at LHC and precise 1-loop low energy data, J. High Energy Phys. 07 (2012) 038.

[39] S. Das, F. Deppisch, O. Kittel, and J. Valle, Heavy neutrinos and lepton flavour violation in left-right symmetric models at the LHC, Phys. Rev. D **86**, 055006 (2012).

[40] J. A. Aguilar-Saavedra and F. R. Joaquim, Measuring heavy neutrino couplings at the LHC, Phys. Rev. D **86**, 073005 (2012).

[41] T. Han, I. Lewis, R. Ruiz, and Z.-g. Si, Lepton number violation and W' chiral couplings at the LHC, Phys. Rev. D **87**, 035011 (2013); **87**, 039906(E) (2013).
[42] C.-Y. Chen, P. S. B. Dev, and R. N. Mohapatra, Probing heavy-light neutrino mixing in left-right seesaw models at the LHC, Phys. Rev. D **88**, 033014 (2013).
[43] T. G. Rizzo, Exploring new gauge bosons at a 100 TeV collider, Phys. Rev. D **89**, 095022 (2014).
[44] F. F. Deppisch, T. E. Gonzalo, S. Patra, N. Sahu, and U. Sarkar, Double beta decay, lepton flavor violation, and collider signatures of left-right symmetric models with spontaneous D-parity breaking, Phys. Rev. D **91**, 015018 (2015).
[45] F. F. Deppisch, P. S. Bhupal Dev, and A. Pilaftsis, Neutrinos and collider physics, New J. Phys. **17**, 075019 (2015).
[46] J. Gluza and T. Jeliński, Heavy neutrinos and the $pp \to lljj$ CMS data, Phys. Lett. B **748**, 125 (2015).
[47] J. N. Ng, A. de la Puente, and B. W.-P. Pan, Search for heavy right-handed neutrinos at the LHC and beyond in the same-sign same-flavor leptons final state, J. High Energy Phys. 12 (2015) 172.
[48] S. Patra, F. S. Queiroz, and W. Rodejohann, Stringent dilepton bounds on left-right models using LHC data, Phys. Lett. B **752**, 186 (2016).
[49] B. A. Dobrescu and Z. Liu, W' Boson Near 2 TeV: Predictions for Run 2 of the LHC, Phys. Rev. Lett. **115**, 211802 (2015).
[50] J. Brehmer, J. Hewett, J. Kopp, T. Rizzo, and J. Tattersall, Symmetry restored in dibosons at the LHC?, J. High Energy Phys. 10 (2015) 182.
[51] P. S. Bhupal Dev and R. N. Mohapatra, Unified Explanation of the $eejj$, Diboson and Dijet Resonances at the LHC, Phys. Rev. Lett. **115**, 181803 (2015).
[52] P. Coloma, B. A. Dobrescu, and J. Lopez-Pavon, Right-handed neutrinos and the 2 TeV W' boson, Phys. Rev. D **92**, 115023 (2015).
[53] F. F. Deppisch, L. Graf, S. Kulkarni, S. Patra, W. Rodejohann, N. Sahu, and U. Sarkar, Reconciling the 2 TeV excesses at the LHC in a linear seesaw left-right model, Phys. Rev. D **93**, 013011 (2016).
[54] P. S. B. Dev, D. Kim, and R. N. Mohapatra, Disambiguating seesaw models using invariant mass variables at hadron colliders, J. High Energy Phys. 01 (2016) 118.
[55] S. Mondal and S. K. Rai, Polarized window for left-right symmetry and a right-handed neutrino at the Large Hadron-Electron Collider, Phys. Rev. D **93**, 011702 (2016).
[56] J. A. Aguilar-Saavedra and F. R. Joaquim, Multiboson production in W' decays, J. High Energy Phys. 01 (2016) 183.
[57] M. Lindner, F. S. Queiroz, and W. Rodejohann, Dilepton bounds on left–right symmetry at the LHC run II and neutrinoless double beta decay, Phys. Lett. B **762**, 190 (2016).
[58] M. Lindner, F. S. Queiroz, W. Rodejohann, and C. E. Yaguna, Left-right symmetry and lepton number violation at the large hadron electron collider, J. High Energy Phys. 06 (2016) 140.
[59] M. Mitra, R. Ruiz, D. J. Scott, and M. Spannowsky, Neutrino jets from high-mass W_R gauge bosons in TeV-scale left-right symmetric models, Phys. Rev. D **94**, 095016 (2016).
[60] G. Anamiati, M. Hirsch, and E. Nardi, Quasi-Dirac neutrinos at the LHC, J. High Energy Phys. 10 (2016) 010.
[61] V. Khachatryan *et al.* (CMS Collaboration), Search for heavy neutrinos and W bosons with right-handed couplings in proton-proton collisions at $\sqrt{s} = 8$ TeV, Eur. Phys. J. C **74**, 3149 (2014).
[62] G. Aad *et al.* (ATLAS Collaboration), Search for heavy Majorana neutrinos with the ATLAS detector in pp collisions at $\sqrt{s} = 8$ TeV, J. High Energy Phys. 07 (2015) 162.
[63] V. Khachatryan *et al.* (CMS Collaboration), Search for heavy neutrinos or third-generation leptoquarks in final states with two hadronically decaying tau leptons and two jets in proton-proton collisions at sqrt(s) = 13 TeV, J. High Energy Phys. 03 (2017) 077.
[64] M. Hirsch, S. Morisi, and J. W. F. Valle, A4-based tri-bimaximal mixing within inverse and linear seesaw schemes, Phys. Lett. B **679**, 454 (2009).
[65] P.-H. Gu and U. Sarkar, Leptogenesis with linear, inverse or double seesaw, Phys. Lett. B **694**, 226 (2011).
[66] P. S. B. Dev and R. N. Mohapatra, TeV scale inverse seesaw in SO(10) and leptonic non-unitarity effects, Phys. Rev. D **81**, 013001 (2010).
[67] P. Humbert, M. Lindner, S. Patra, and J. Smirnov, Lepton number violation within the conformal inverse seesaw, J. High Energy Phys. 09 (2015) 064.
[68] M. K. Parida and S. Patra, Left-right models with light neutrino mass prediction and dominant neutrinoless double beta decay rate, Phys. Lett. B **718**, 1407 (2013).
[69] V. Brdar and A. Y. Smirnov, Low scale left-right symmetry and naturally small neutrino mass, J. High Energy Phys. 02 (2019) 045.
[70] M. Thomas Arun, T. Mandal, S. Mitra, A. Mukherjee, L. Priya, and A. Sampath, Testing left-right symmetry with an inverse seesaw mechanism at the LHC, Phys. Rev. D **105**, 115007 (2022).
[71] P. Sahu, S. Patra, and P. Pritimita, Neutrino mass and lepton flavor violation in A_4-based left–right symmetric model with linear seesaw, Int. J. Mod. Phys. A **37**, 2250030 (2022).
[72] K. Ezzat, M. Ashry, and S. Khalil, Search for a heavy neutral Higgs boson in a left-right model with an inverse seesaw mechanism at the LHC, Phys. Rev. D **104**, 015016 (2021).
[73] V. Tello, M. Nemevsek, F. Nesti, G. Senjanovic, and F. Vissani, Left-Right Symmetry: From LHC to Neutrinoless Double Beta Decay, Phys. Rev. Lett. **106**, 151801 (2011).
[74] J. Barry and W. Rodejohann, Lepton number and flavour violation in TeV-scale left-right symmetric theories with large left-right mixing, J. High Energy Phys. 09 (2013) 153.
[75] P. S. Bhupal Dev, S. Goswami, M. Mitra, and W. Rodejohann, Constraining neutrino mass from neutrinoless double beta decay, Phys. Rev. D **88**, 091301 (2013).

[76] A. E. C. Hernández and I. Schmidt, A renormalizable left-right symmetric model with low scale seesaw mechanisms, Nucl. Phys. **B976**, 115696 (2022).
[77] V. Brdar, L. Graf, A. J. Helmboldt, and X.-J. Xu, Gravitational waves as a probe of left-right symmetry breaking, J. Cosmol. Astropart. Phys. 12 (2019) 027.
[78] A. Maiezza, M. Nemevsek, F. Nesti, and G. Senjanovic, Left-right symmetry at LHC, Phys. Rev. D **82**, 055022 (2010).
[79] A. Y. Smirnov, Seesaw enhancement of lepton mixing, Phys. Rev. D **48**, 3264 (1993).
[80] G. Altarelli and F. Feruglio, Models of neutrino masses and mixings, New J. Phys. **6**, 106 (2004).
[81] M. Lindner, M. A. Schmidt, and A. Y. Smirnov, Screening of Dirac flavor structure in the seesaw and neutrino mixing, J. High Energy Phys. 07 (2005) 048.
[82] P. O. Ludl and A. Y. Smirnov, Lepton mixing from the hidden sector, Phys. Rev. D **92**, 073010 (2015).
[83] B. Bajc and A. Y. Smirnov, Hidden flavor symmetries of SO(10) GUT, Nucl. Phys. **B909**, 954 (2016).
[84] A. Y. Smirnov and X.-J. Xu, Neutrino mixing in SO(10) GUTs with a non-Abelian flavor symmetry in the hidden sector, Phys. Rev. D **97**, 095030 (2018).
[85] B. Pontecorvo, Inverse beta processes and nonconservation of lepton charge, Zh. Eksp. Teor. Fiz. **34**, 247 (1957).
[86] Z. Maki, M. Nakagawa, and S. Sakata, Remarks on the unified model of elementary particles, Prog. Theor. Phys. **28**, 870 (1962).
[87] B. Pontecorvo, Neutrino experiments and the problem of conservation of leptonic charge, Zh. Eksp. Teor. Fiz. **53**, 1717 (1967).
[88] M. Tanabashi *et al.* (Particle Data Group), Review of particle physics, Phys. Rev. D **98**, 030001 (2018).
[89] S. M. Bilenky, J. Hosek, and S. T. Petcov, On oscillations of neutrinos with Dirac and Majorana masses, Phys. Lett. **94B**, 495 (1980).
[90] F. Capozzi, E. Di Valentino, E. Lisi, A. Marrone, A. Melchiorri, and A. Palazzo, Addendum to global constraints on absolute neutrino masses and their ordering, Phys. Rev. D **101**, 116013 (2020).
[91] M. Aaboud *et al.* (ATLAS Collaboration), Search for heavy Majorana or Dirac neutrinos and right-handed W gauge bosons in final states with two charged leptons and two jets at $\sqrt{s} = 13$ TeV with the ATLAS detector, J. High Energy Phys. 01 (2019) 016.
[92] M. Aaboud *et al.* (ATLAS Collaboration), Search for a right-handed gauge boson decaying into a high-momentum heavy neutrino and a charged lepton in pp collisions with the ATLAS detector at $\sqrt{s} = 13$ TeV, Phys. Lett. B **798**, 134942 (2019).
[93] A. M. Sirunyan *et al.* (CMS Collaboration), Search for a heavy right-handed W boson and a heavy neutrino in events with two same-flavor leptons and two jets at $\sqrt{s} = 13$ TeV, J. High Energy Phys. 05 (2018) 148.
[94] T. Li, X.-D. Ma, and M. A. Schmidt, Constraints on the charged currents in general neutrino interactions with sterile neutrinos, J. High Energy Phys. 10 (2020) 115.
[95] W. Dekens, L. Andreoli, J. de Vries, E. Mereghetti, and F. Oosterhof, A low-energy perspective on the minimal left-right symmetric model, J. High Energy Phys. 11 (2021) 127.
[96] M. Doi, T. Kotani, and E. Takasugi, Double beta decay and Majorana neutrino, Prog. Theor. Phys. Suppl. **83**, 1 (1985).
[97] A. Halprin, S. T. Petcov, and S. P. Rosen, Effects of light and heavy Majorana neutrinos in neutrinoless double beta decay, Phys. Lett. **125B**, 335 (1983).
[98] A. Faessler, A. Meroni, S. T. Petcov, F. Simkovic, and J. Vergados, Uncovering multiple CP-nonconserving mechanisms of $(\beta\beta)_{0\nu}$ decay, Phys. Rev. D **83**, 113003 (2011).
[99] H. Ejiri, J. Suhonen, and K. Zuber, Neutrino–nuclear responses for astro-neutrinos, single beta decays and double beta decays, Phys. Rep. **797**, 1 (2019).
[100] M. Horoi and A. Neacsu, Towards an effective field theory approach to the neutrinoless double-beta decay, arXiv:1706.05391.
[101] D.-L. Fang, A. Faessler, and F. Simkovic, $0\nu\beta\beta$ -decay nuclear matrix element for light and heavy neutrino mass mechanisms from deformed quasiparticle random-phase approximation calculations for ^{76}Ge, ^{82}Se, ^{130}Te, ^{136}Xe, and ^{150}Nd with isospin restoration, Phys. Rev. C **97**, 045503 (2018).
[102] F. Šimkovic, V. Rodin, A. Faessler, and P. Vogel, $0\nu\beta\beta$ and $2\nu\beta\beta$ nuclear matrix elements, quasiparticle random-phase approximation, and isospin symmetry restoration, Phys. Rev. C **87**, 045501 (2013).
[103] A. Faessler, M. González, S. Kovalenko, and F. Šimkovic, Arbitrary mass Majorana neutrinos in neutrinoless double beta decay, Phys. Rev. D **90**, 096010 (2014).
[104] J. Hyvärinen and J. Suhonen, Nuclear matrix elements for $0\nu\beta\beta$ decays with light or heavy Majorana-neutrino exchange, Phys. Rev. C **91**, 024613 (2015).
[105] J. Barea, J. Kotila, and F. Iachello, Nuclear matrix elements for double-β decay, Phys. Rev. C **87**, 014315 (2013).
[106] L. S. Song, J. M. Yao, P. Ring, and J. Meng, Relativistic description of nuclear matrix elements in neutrinoless double-β decay, Phys. Rev. C **90**, 054309 (2014).
[107] J. M. Yao, L. S. Song, K. Hagino, P. Ring, and J. Meng, Systematic study of nuclear matrix elements in neutrinoless double-β decay with a beyond-mean-field covariant density functional theory, Phys. Rev. C **91**, 024316 (2015).
[108] L. S. Song, J. M. Yao, P. Ring, and J. Meng, Nuclear matrix element of neutrinoless double-β decay: Relativity and short-range correlations, Phys. Rev. C **95**, 024305 (2017).
[109] J. Menéndez, Neutrinoless $\beta\beta$ decay mediated by the exchange of light and heavy neutrinos: The role of nuclear structure correlations, J. Phys. G **45**, 014003 (2018).
[110] S. M. Bilenky and S. T. Petcov, Massive neutrinos and neutrino oscillations, Rev. Mod. Phys. **59**, 671 (1987); **61**, 169(E) (1989); **60**, 575(E) (1988).
[111] V. Cirigliano, W. Dekens, J. De Vries, M. L. Graesser, E. Mereghetti, S. Pastore, and U. Van Kolck, New Leading Contribution to Neutrinoless Double-β Decay, Phys. Rev. Lett. **120**, 202001 (2018).
[112] V. Cirigliano, W. Dekens, J. de Vries, M. Hoferichter, and E. Mereghetti, Toward Complete Leading-Order Predictions for Neutrinoless Double β Decay, Phys. Rev. Lett. **126**, 172002 (2021).

[113] R. Wirth, J. M. Yao, and H. Hergert, *Ab Initio* Calculation of the Contact Operator Contribution in the Standard Mechanism for Neutrinoless Double Beta Decay, Phys. Rev. Lett. **127**, 242502 (2021).
[114] R. Weiss, P. Soriano, A. Lovato, J. Menendez, and R. B. Wiringa, Neutrinoless double-β decay: Combining quantum Monte Carlo and the nuclear shell model with the generalized contact formalism, Phys. Rev. C **106**, 065501 (2022).
[115] A. Babić, S. Kovalenko, M. I. Krivoruchenko, and F. Šimkovic, Interpolating formula for the $0\nu\beta\beta$-decay half-life in the case of light and heavy neutrino mass mechanisms, Phys. Rev. D **98**, 015003 (2018).
[116] S. I. Alvis *et al.* (Majorana Collaboration), A search for neutrinoless double-beta decay in ^{76}Ge with 26 kg-yr of exposure from the MAJORANA DEMONSTRATOR, Phys. Rev. C **100**, 025501 (2019).
[117] I. J. Arnquist *et al.* (Majorana Collaboration), Final Result of the MAJORANA DEMONSTRATOR's Search for Neutrinoless Double-β Decay in ^{76}Ge, Phys. Rev. Lett. **130**, 062501 (2023).
[118] O. Azzolini *et al.*, Final Result of CUPID-0 Phase-I in the Search for the ^{82}Se Neutrinoless Double-β Decay, Phys. Rev. Lett. **123**, 032501 (2019).
[119] D. Q. Adams *et al.* (CUORE Collaboration), Search for Majorana neutrinos exploiting millikelvin cryogenics with CUORE, Nature (London) **604**, 53 (2022).
[120] J. de Vries, G. Li, M. J. Ramsey-Musolf, and J. C. Vasquez, Light sterile neutrinos, left-right symmetry, and $0\nu\beta\beta\beta$ decay, J. High Energy Phys. 11 (2022) 056.
[121] S. Pascoli and S. T. Petcov, The SNO solar neutrino data, neutrinoless double beta decay and neutrino mass spectrum, Phys. Lett. B **544**, 239 (2002).
[122] S. Pascoli, S. T. Petcov, and L. Wolfenstein, Searching for the *CP* violation associated with Majorana neutrinos, Phys. Lett. B **524**, 319 (2002).
[123] S. Pascoli, S. T. Petcov, and T. Schwetz, The absolute neutrino mass scale, neutrino mass spectrum, majorana *CP*-violation and neutrinoless double-beta decay, Nucl. Phys. **B734**, 24 (2006).
[124] P. D. Bolton, F. F. Deppisch, and P. S. Bhupal Dev, Neutrinoless double beta decay versus other probes of heavy sterile neutrinos, J. High Energy Phys. 03 (2020) 170.
[125] J. T. Penedo and S. T. Petcov, The 10^{-3} eV frontier in neutrinoless double beta decay, Phys. Lett. B **786**, 410 (2018).
[126] S. Vagnozzi, E. Giusarma, O. Mena, K. Freese, M. Gerbino, S. Ho, and M. Lattanzi, Unveiling ν secrets with cosmological data: Neutrino masses and mass hierarchy, Phys. Rev. D **96**, 123503 (2017).
[127] P. A. Zyla *et al.* (Particle Data Group), Review of particle physics, Prog. Theor. Exp. Phys. **2020**, 083C01 (2020).
[128] F. Capozzi, E. Di Valentino, E. Lisi, A. Marrone, A. Melchiorri, and A. Palazzo, Global constraints on absolute neutrino masses and their ordering, Phys. Rev. D **95**, 096014 (2017); **101**, 116013(A) (2020).
[129] M. Aker *et al.* (KATRIN Collaboration), Improved Upper Limit on the Neutrino Mass from a Direct Kinematic Method by KATRIN, Phys. Rev. Lett. **123**, 221802 (2019).
[130] A. Giuliani, J. J. Gomez Cadenas, S. Pascoli, E. Previtali, R. Saakyan, K. Schäffner, and S. Schönert (APPEC Committee), Double beta decay APPEC Committee Report, arXiv:1910.04688.
[131] M. Agostini, G. Benato, J. A. Detwiler, J. Menéndez, and F. Vissani, Toward the discovery of matter creation with neutrinoless double-beta decay, arXiv:2202.01787.
[132] L. Calibbi and G. Signorelli, Charged lepton flavour violation: An experimental and theoretical introduction, Riv. Nuovo Cimento **41**, 71 (2018).
[133] J. C. Helo, M. Hirsch, and S. Kovalenko, Heavy neutrino searches at the LHC with displaced vertices, Phys. Rev. D **89**, 073005 (2014); **93**, 099902(E) (2016).
[134] E. Izaguirre and B. Shuve, Multilepton and lepton jet probes of sub-weak-scale right-handed neutrinos, Phys. Rev. D **91**, 093010 (2015).
[135] G. Aad *et al.* (ATLAS Collaboration), Search for a Light Higgs Boson Decaying to Long-Lived Weakly-Interacting Particles in Proton-Proton Collisions at $\sqrt{s} = 7$ TeV with the ATLAS Detector, Phys. Rev. Lett. **108**, 251801 (2012).
[136] S. Chatrchyan *et al.* (CMS Collaboration), Searches for long-lived charged particles in pp collisions at $\sqrt{s} = 7$ and 8 TeV, J. High Energy Phys. 07 (2013) 122.
[137] G. Aad *et al.* (ATLAS Collaboration), Search for displaced muonic lepton jets from light Higgs boson decay in proton-proton collisions at $\sqrt{s} = 7$ TeV with the ATLAS detector, Phys. Lett. B **721**, 32 (2013).
[138] F. M. L. Almeida, Jr., Y. do Amaral Coutinho, J. A. Martins Simoes, and M. A. B. do Vale, On a signature for heavy Majorana neutrinos in hadronic collisions, Phys. Rev. D **62**, 075004 (2000).